iScience

CellPress
OPEN ACCESS

Article

GSDME-Dependent Incomplete Pyroptosis Permits Selective IL-1α Release under Caspase-1 Inhibition

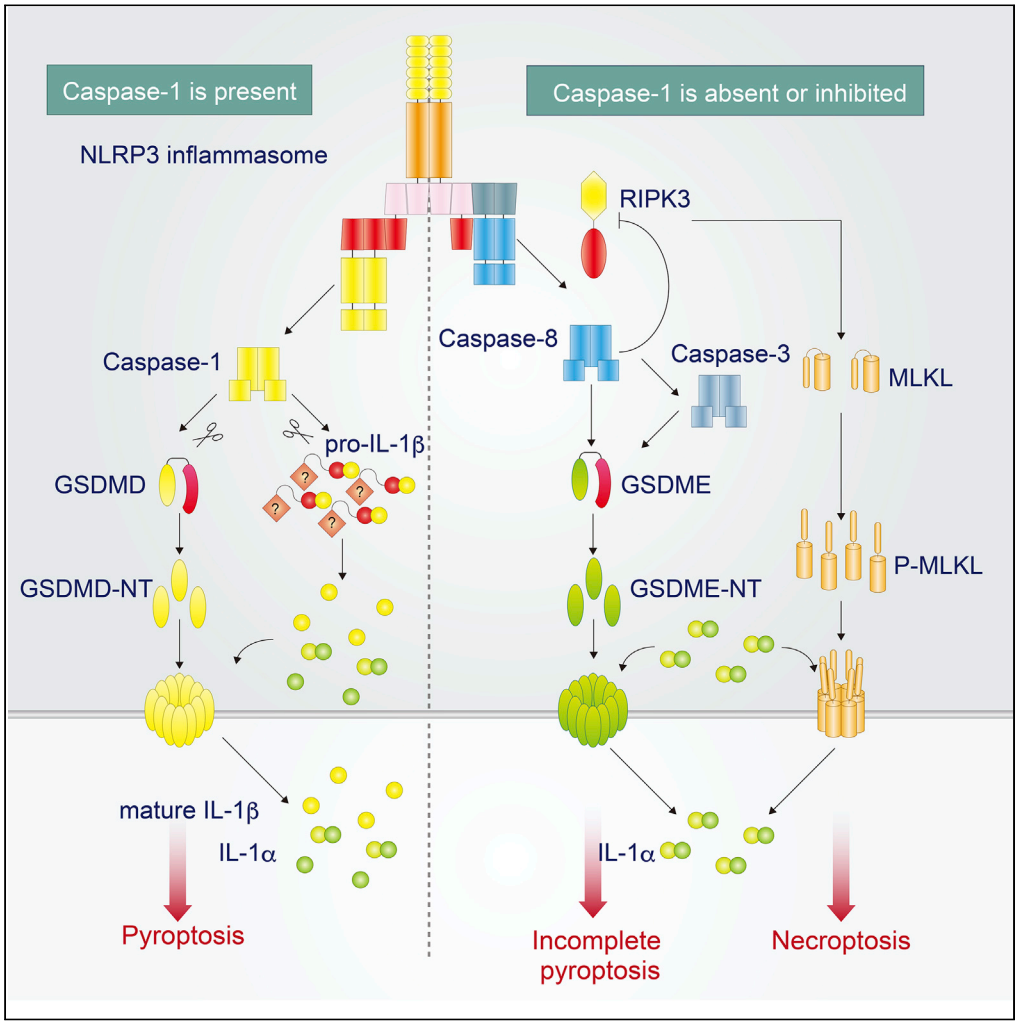

Emi Aizawa, Tadayoshi Karasawa, Sachiko Watanabe, ..., Tadashi Kasahara, Yoshiyuki Mori, Masafumi Takahashi

tdys.karasawa@jichi.ac.jp (T.K.)
masafumi2@jichi.ac.jp (M.T.)

HIGHLIGHTS

NLRP3 inflammasome induces necrotic cell death in the absence of caspase-1/11

ASC initiates GSDME-dependent pyroptosis via caspase-8

IL-1α, but not IL-1β, is released during Casp1/11-independent pyroptosis

Pharmacological inhibition of caspase-1 permits IL-1α release during pyroptosis

Aizawa et al., iScience *23*, 101070
May_22, 2020
https://doi.org/10.1016/j.isci.2020.101070

iScience

CellPress
OPEN ACCESS

Article

GSDME-Dependent Incomplete Pyroptosis Permits Selective IL-1α Release under Caspase-1 Inhibition

Emi Aizawa,[1,2,3] Tadayoshi Karasawa,[1,3,4,*] Sachiko Watanabe,[1] Takanori Komada,[1] Hiroaki Kimura,[1] Ryo Kamata,[1] Homare Ito,[1] Erika Hishida,[1] Naoya Yamada,[1] Tadashi Kasahara,[1] Yoshiyuki Mori,[2] and Masafumi Takahashi[1,*]

SUMMARY

Pyroptosis is a form of regulated cell death that is characterized by gasdermin processing and increased membrane permeability. Caspase-1 and caspase-11 have been considered to be essential for gasdermin D processing associated with inflammasome activation. In the present study, we found that NLRP3 inflammasome activation induces delayed necrotic cell death via ASC in caspase-1/11-deficient macrophages. Furthermore, ASC-mediated caspase-8 activation and subsequent gasdermin E processing are necessary for caspase-1-independent necrotic cell death. We define this necrotic cell death as incomplete pyroptosis because IL-1β release, a key feature of pyroptosis, is absent, whereas IL-1α release is induced. Notably, unprocessed pro-IL-1β forms a molecular complex to be retained inside pyroptotic cells. Moreover, incomplete pyroptosis accompanied by IL-1α release is observed under the pharmacological inhibition of caspase-1 with VX765. These findings suggest that caspase-1 inhibition during NLRP3 inflammasome activation modulates forms of cell death and permits the release of IL-1α from dying cells.

INTRODUCTION

Necrotic cell death associated with various diseases, including myocardial infarction, acute kidney injury, neurodegeneration, and diabetes, triggers inflammatory responses to promote the progression of disease and tissue repair (Tonnus and Linkermann, 2017; Tonnus et al., 2019). Besides accidental necrotic cell death, intrinsic cell mechanisms induce regulated cell death (RCD) to regulate post-injury inflammation (Martin, 2016; Vanden Berghe et al., 2014). Apoptosis, the most extensively studied RCD, is regarded as an anti-inflammatory cell death because it has minimum effects on neighboring cells (Martin et al., 2012). In contrast, necrosis and necrotic RCD can cause inflammation by releasing various damage/danger-associated molecular patterns (DAMPs), such as adenosine triphosphate (ATP), dsDNA, ssRNA, and high-mobility group box 1 (HMGB1), from dying cells (Martin et al., 2012). Thus, regulation of RCD could be a potential target for modulating post-injury inflammation. Meanwhile, the released DAMPs in turn activate pattern recognition receptors (PRRs), which are expressed in innate immune cells and induce subsequent inflammatory responses (Bertheloot and Latz, 2017; Martin et al., 2012). Among PRRs, a group of receptors, including nucleotide-binding oligomerization domain, leucine-rich repeat and pyrin domain containing 3 (NLRP3), NLR and caspase recruitment domain containing 4 (NLRC4), and absent in melanoma 2 (AIM2), form an inflammasome assembly to induce subsequent inflammatory responses through the activation of caspase-1 (Karasawa and Takahashi, 2017; Lamkanfi and Dixit, 2014).

NLRP3 is mainly expressed in innate immune cells such as macrophages and forms "NLRP3 inflammasome" with apoptosis-associated speck-like protein containing a caspase recruitment domain (ASC), which functions as an adaptor protein, and a cysteine proteinase caspase-1 (Karasawa and Takahashi, 2017; Lamkanfi and Dixit, 2014). In response to pathogen-associated molecular patterns (PAMPs) or DAMPs, the components of NLRP3 inflammasome assemble to activate caspase-1, and the active caspase-1 then processes a potent inflammatory cytokine interleukin (IL)-1β into its mature form (Lamkanfi and Dixit, 2014). Similarly, IL-1α, another cytokine belonging to the IL-1 family, is released during NLRP3 inflammasome activation, although it is not directly processed by caspase-1 (Gross et al., 2012). Furthermore, the active caspase-1 induces an inflammatory RCD called pyroptosis (Karasawa and Takahashi, 2017; Lamkanfi and Dixit, 2014).

[1]Division of Inflammation Research, Center for Molecular Medicine, Jichi Medical University, 3311-1 Yakushiji, Shimotsuke, Tochigi 329-0498, Japan

[2]Department of Dentistry, Oral and Maxillofacial Surgery, Jichi Medical University, Tochigi, Japan

[3]These authors contributed equally

[4]Lead Contact

*Correspondence: tdys.karasawa@jichi.ac.jp (T.K.), masafumi2@jichi.ac.jp (M.T.)

https://doi.org/10.1016/j.isci.2020.101070

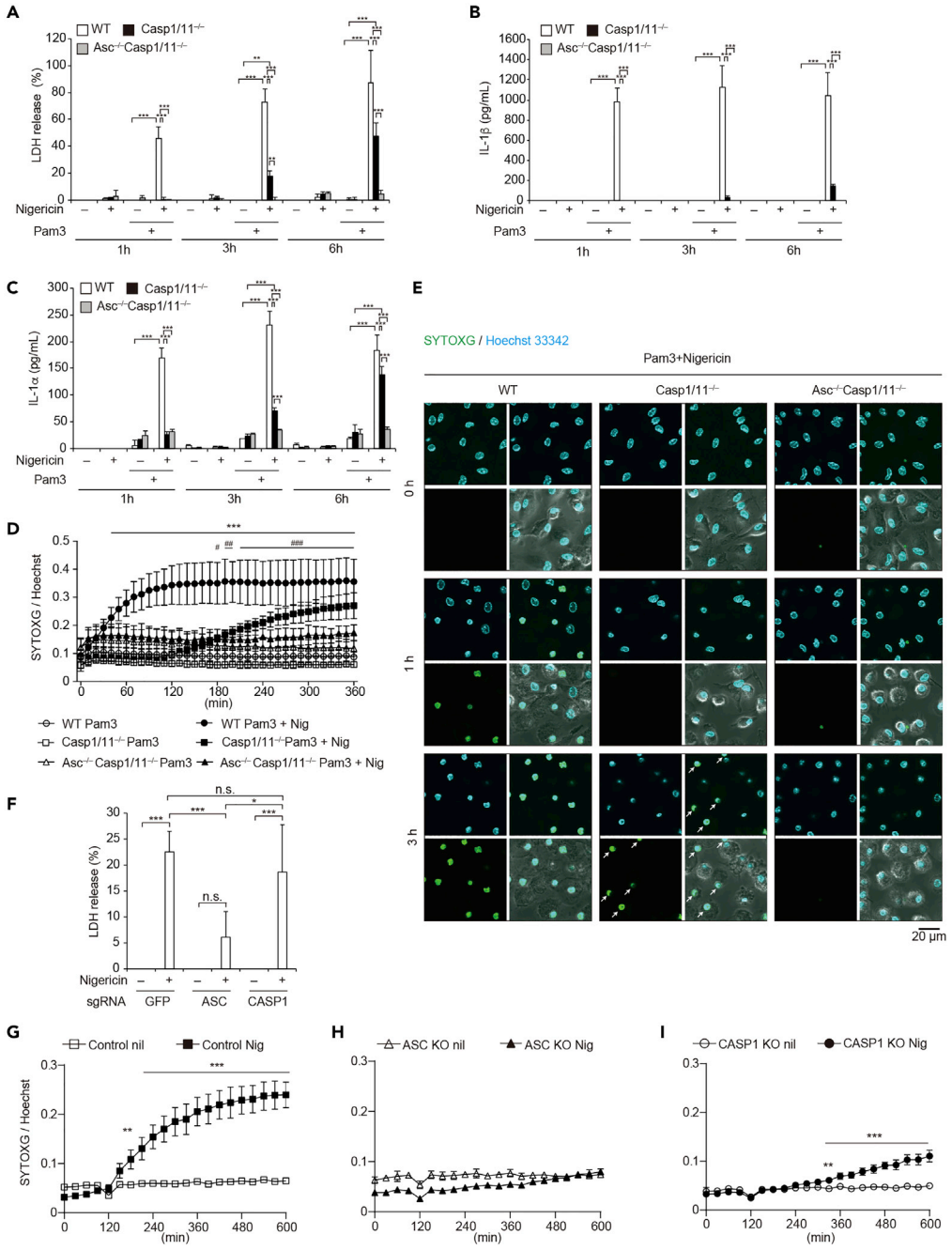

Figure 1. Nigericin Induces Caspase-1/11-Independent Necrotic Cell Death via ASC

(A–C) Primary peritoneal macrophages isolated from WT, *Casp1/11*$^{-/-}$, and *Asc*$^{-/-}$ *Casp1/11*$^{-/-}$ mice were rested or primed with Pam3CSK4 (100 ng/mL) for 18 h and then treated with nigericin (5 μM) for 1, 3, or 6 h. (A) The levels of LDH in the supernatants were assessed. (B) The levels of IL-1β and (C) IL-1α in the supernatants were assessed by ELISA.

(D and E) Primed WT, *Casp1/11*$^{-/-}$, and *Asc*$^{-/-}$ *Casp1/11*$^{-/-}$ macrophages were labeled with Hoechst33342 and then treated with nigericin in the presence of SYTOXG. (D) Relative fluorescence units of SYTOXG were measured at 10-min intervals. (E) Images of Hoechst staining (upper left), SYTOXG staining (bottom left), merged images of Hoechst and SYTOXG (upper right), and merged images of fluorescent and bright fields (bottom right) were visualized by confocal microscopy. White arrows indicate dead *Casp1/11*$^{-/-}$ macrophages.

(F–I) Control, *ASC* KO, and *CASP1* KO THP-1 cells were differentiated with PMA for 48 h and then treated with nigericin (5 μM). (F) The levels of LDH in the supernatants 8 h after nigericin stimulation were assessed. (G) Relative fluorescence units of SYTOXG in (G) Control, (H), *ASC* KO, (I) and *CASP1*KO THP1 cells were measured at 30-min intervals.

Figure 1. *Continued*

Data represent mean ± SD of three (A and D) or four (F) independent experiments. (B, C, and G–I) Data are shown as mean ± SD of triplicate of one experiment. (B, C, E, and G–I) Data are representative of two independent experiments. (A–C, F, G, I) *p < 0.05, **p < 0.01, ***p < 0.001 as determined by two-way ANOVA with a post hoc test. (D) ***p < 0.001 compared with WT Pam3 and WT Pam3+Nig, #p < 0.05, ##p < 0.01, ###p < 0.001 compared with *Casp1/11*$^{-/-}$ Pam3 and *Casp1/11*$^{-/-}$ Pam3+Nig as determined by two-way ANOVA with a post hoc test. n.s., not significant.

Among RCDs, pyroptosis is a highly inflammatory cell death that is initiated by inflammatory caspases. Through caspase activation, pyroptotic cells show both apoptotic and necrotic characteristics (Miao et al., 2011). The former includes DNA fragmentation and chromatin condensation, and blebbing. Furthermore, pyroptosis is accompanied by increased membrane permeability, cell swelling, and release of cytosolic content, which is characterized by lactate dehydrogenase (LDH) release. Inflammatory caspases including caspase-1, caspase-4, and caspase-5 have been identified as initiators of pyroptosis in humans. In addition to murine caspase-1, caspase-11, a homolog of caspase-4 and -5 in mice, can initiate pyroptosis. Recent studies have revealed that the executor of pyroptosis mediated by inflammatory caspases is GSDMD (Kayagaki et al., 2015; Shi et al., 2015). GSDMD is a member of the gasdermin family, including GSDMA, B, C, D, E and DFNB59, which share a similar structure (Ding et al., 2016). An amino-terminal domain (NT) of GSDMD possesses pore-forming activity, whereas the carboxy-terminal domain exerts an autoinhibitory effect against NT. After caspase-mediated cleavage of linker domain, NT of GSDMD oligomerizes in plasma membrane where it is enriched with phosphatidylinositol phosphates and forms pores of 13–22 nm (Ding et al., 2016; Liu et al., 2016). The GSDMD-formed pore in turn induces the release of cytosolic content including LDH and IL-1α/β. Since pyroptosis is a highly inflammatory form of cell death (Miao et al., 2011), the modulation of pyroptosis during NLRP3 inflammasome activation is expected to be effective for preventing inflammatory disorders.

The activation of the NLRP3 inflammasome promotes not only caspase-1 activation but also caspase-8 activation as an alternative effector (Antonopoulos et al., 2015) because assembled ASC can be a scaffold for caspase-8 via pyrin domain (Vajjhala et al., 2015). The activated caspase-8 by NLRP3 inflammasome under caspase-1 inhibition is involved in two distinct functions: IL-1β processing and induction of apoptosis via caspase-3 (Antonopoulos et al., 2015). Therefore, inflammasome activation in the absence of caspase-1 induces anti-inflammatory apoptotic cell death (Sagulenko et al., 2013), indicating that caspase-1 inhibition could be a target to convert the form of cell death from pyroptosis to apoptosis. However, other reports suggest that inflammasome activation induces necrotic cell death independent of caspase-1 (Motani et al., 2011; Satoh et al., 2013; Schneider et al., 2017). Thus, the precise mechanisms and the form of cell death induced by NLRP3 inflammasome activation under caspase-1 inhibition remain unclear. In the present study, we characterized necrotic cell death induced by NLRP3 inflammasome activation independent of caspase-1 and -11 (caspase-1/11) and determined that GSDME is involved in this process. We further found that this necrotic cell death is incomplete pyroptosis, which occurs without IL-1β release.

RESULTS

Nigericin Induces Caspase-1/11-Independent Necrotic Cell Death via ASC

To investigate whether NLRP3 inflammasome activation induces necrotic cell death independent of caspase-1/11, wild-type (WT), NLRP3 knockout (*Nlrp3*$^{-/-}$), or caspase-1 and caspase-11 double-knockout (*Casp1/11*$^{-/-}$) peritoneal macrophages were primed with Pam3CSK4 for 18 h and then stimulated with nigericin, a potent NLRP3 inflammasome activator. LDH release was induced immediately after nigericin stimulation in WT macrophages, whereas the response was inhibited in both *Nlrp3*$^{-/-}$ and *Casp1/11*$^{-/-}$ macrophages (Figures S1A and S1B). At later time point, however, LDH release was detected from *Casp1/11*$^{-/-}$ macrophages, indicating that NLRP3 inflammasome induces caspase-1/11-independent cell death. Since ASC is an essential scaffold for signal transduction mediated by NLRP3 inflammasome (Lamkanfi and Dixit, 2014), *Casp1/11*$^{-/-}$ mice were crossed with ASC knockout (*Asc*$^{-/-}$) mice to investigate the role of ASC in caspase-1/11-independent necrotic cell death. Indeed, nigericin-induced LDH release at later time point was canceled in *Asc*$^{-/-}$ *Casp1/11*$^{-/-}$ macrophages (Figure 1A). As expected, IL-1β release was completely inhibited from both *Casp1/11*$^{-/-}$ macrophages and *Asc*$^{-/-}$ *Casp1/11*$^{-/-}$ macrophages even at a later time point (Figure 1B). Notably, a substantial amount of IL-1α release was detected from *Casp1/11*$^{-/-}$ macrophages, whereas IL-1α release was also canceled in *Asc*$^{-/-}$ *Casp1/11*$^{-/-}$ macrophages (Figure 1C). To investigate the precise time course of nigericin-induced necrotic cell death in *Casp1/11*$^{-/-}$ macrophages, we used SYTOX green (SYTOXG) staining assay with real-time monitoring of dead cells. In WT

macrophages, SYTOXG fluorescence started to increase 40 min after nigericin stimulation (Figure 1D). On the other hand, cell death in *Casp1/11*$^{-/-}$ macrophages began 180 min after stimulation. This delayed cell death was also visualized by confocal microscopy (Figure 1E, indicated by white arrows). Although cell swelling, a key morphological change during pyroptosis, was observed in both WT and *Casp1/11*$^{-/-}$ macrophages, nuclei of *Casp1/11*$^{-/-}$ macrophages were more condensed than those of WT macrophages (Figures S1C–S1E). Although we tested the effect of priming duration on caspase-1-independent necrotic cell death, the capability of the necrotic cell death was reduced in *Casp1/11*$^{-/-}$ macrophages primed with Pam3CSK4 for 4 h (Figures S2A–S2E). Next, we assessed whether similar responses could be observed in other types of macrophages and confirmed that caspase-1/11-independent necrotic cell death was observed in bone marrow-derived macrophages (Figure S2F). Caspase-1-independent necrotic cell death was also assessed in THP-1 cells, which are a human monocytic cell line that can differentiate into macrophages. Similar to murine macrophages, nigericin-induced LDH release was observed in *CASP1* KO THP1 cells, but not in *ASC* KO THP-1 cells (Figures 1F and S2G). Similar trends were confirmed by an SYTOXG assay (Figures 1G–1I, S1F, and S1G). Unlike nigericin, lysosome-damaging stimuli such as cholesterol crystals, palmitic acid crystals, and nanosilica particles induced necrotic cell death in both *CASP1* KO and *ASC* KO THP-1 cells (Figure S2H).

NLRP3 Inflammasome Activation Induces Necrotic Cell Death in the Absence of Caspase-1

To exclude the possibility that nigericin exerted non-specific cytotoxicity, we developed THP-1 cells expressing a NLRP3D303N mutant under the TET-ON promoter (*NLRP3D303N*-THP-1 cells; Figure S3A). NLRP3D303N is a causative mutation of cryopyrin-associated periodic syndromes and is constitutively active. Indeed, doxycycline (DOX)-induced NLRP3D303N expression led to subsequent release of LDH and IL-1β (Figures S3B–S3D). Increased membrane permeability by NLRP3 inflammasome activation was further confirmed by flow cytometry analysis with annexin V and 7-AAD staining (Figure S3E). Next, we produced *ASC* KO or *CASP1* KO *NLRP3D303N* -THP-1 cells. DOX-mediated inflammasome activation characterized by caspase-1 activation was prevented in both *ASC* KO and *CASP1* KO THP-1 cells (Figure 2A). Similar to nigericin-induced LDH release, inflammasome activation-mediated delayed LDH release was detected in *CASP1* KO cells, whereas LDH release was completely prevented in *ASC* KO cells (Figure 2B). To visualize a loss of cytosolic content during pyroptosis, the developed *NLRP3D303N* -THP-1 cells also expressed fluorescent humanized Kusabira Orange (hKO1) protein (Figure S3A). A loss of cytosolic contents and increased membrane permeability during pyroptosis in control cells were successfully visualized with hKO1 and SYTOXG (Figures 2C and S3F). The delayed necrotic cell death in *CASP1* KO cells was also confirmed by loss of hKO1 and SYTOXG staining 18 h after DOX treatment. In addition, necrotic cell death in *CASP1*KO cells was brought about after apoptosis-like morphological changes such as nuclear condensation and shrinkage (Figures 2D and S3G). Furthermore, the onset of cell death was determined using SYTOXG. In control cells, cell death as indicated by SYTOXG fluorescence was increased 4 h after DOX treatment (Figure 2E). Consistent with the LDH assay, SYTOXG fluorescence was significantly increased 16 h after DOX treatment in *CASP1* KO cells, whereas it was unchanged in *ASC* KO cells (Figures 2F and 2G).

Other Caspases Are Involved in Caspase-1/11-Independent Necrotic Cell Death Induced by NLRP3 Inflammasome Activation

Caspase-8 functions as an initiator caspase in *Casp1/11*$^{-/-}$ cells during NLRP3 inflammasome activation (Antonopoulos et al., 2015). Thus, we postulated that inhibition of other caspases could prevent caspase-1/11-independent necrotic cell death induced by NLRP3 inflammasome activation. Indeed, NLRP3 inflammasome-mediated necrotic cell death in the absence of caspase-1 was prevented by a pan-caspase inhibitor Z-VAD (Figures 3A and S4A–S4C). Dead cell monitoring with SYTOXG revealed that the onset of cell death was delayed by Z-VAD treatment in *Casp1/11*$^{-/-}$ macrophages (Figure 3B). This delayed cell death was also confirmed by confocal microscopy (Figure 3C). However, necrotic cell death was detected even in Z-VAD-treated *Casp1/11*$^{-/-}$ macrophages at a later time point (Figures 3B and S4D). Since caspase-8 inactivates receptor-interacting serine-threonine kinase 3 (RIPK3) to prevent necroptosis, the induction of necroptosis in VAD-treated cells is possible (Vanden Berghe et al., 2014). To assess the involvement of necroptosis in this necrotic cell death, a RIPK3 inhibitor GSK'872 was used together with Z-VAD. Combined treatment with Z-VAD and GSK'872 significantly inhibited LDH release and delayed the onset of cell death compared with Z-VAD treatment in *Casp1/11*$^{-/-}$ macrophages (Figures 3D and 3E). In agreement with LDH release, IL-1α release in *Casp1/11*$^{-/-}$ macrophages was substantially induced, and this induction was inhibited by combined treatment with Z-VAD and GSK'872 (Figure 3F). In contrast, IL-1β release was not detected in *Casp1/11* macrophages (Figure 3G). These results suggest

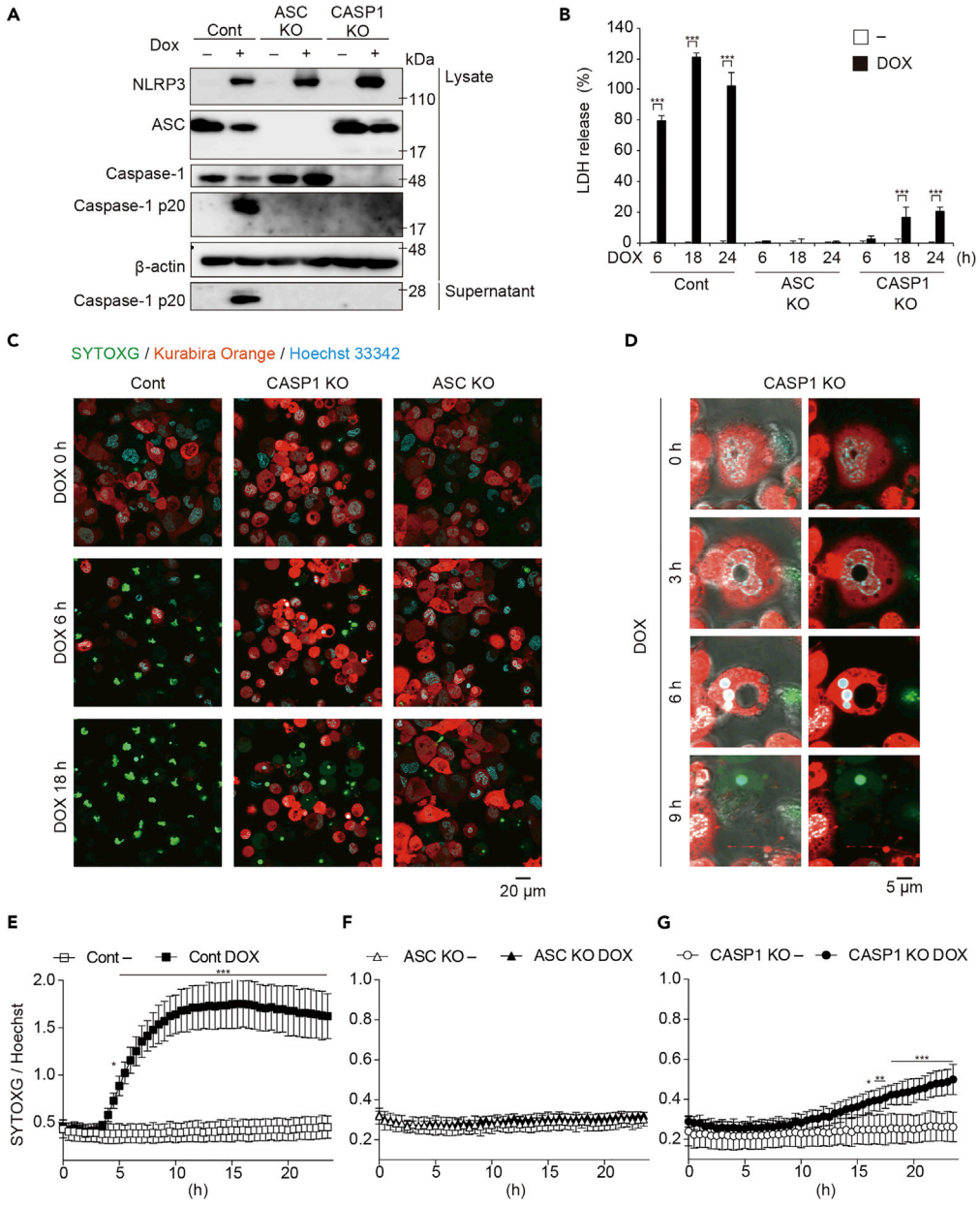

Figure 2. NLRP3 Inflammasome Activation Induces Necrotic Cell Death in the Absence of Caspase-1

(A–F) Control, *ASC* KO, and *CASP1*KO THP1 *NLRP3 D303N* cells were differentiated with PMA for 48 h and then treated with DOX (1 μg/mL). (A) After 6 h, lysates and supernatants were analyzed by western blot. (B) The levels of LDH in the supernatants at the indicated time points were assessed. (C and D) Cells were treated with DOX in the presence of SYTOXG. (C) Merged images of hKO1, SYTOXG, and Hoechst33342 were visualized by confocal microscopy. (D) High-magnification images of DOX-treated *CASP1*KO THP1 *NLRP3 D303N* cells. Images were visualized as merged images of fluorescence (right panels) and merged images of fluorescence and bright fields (left panels).

(E–G) Relative fluorescence units of SYTOXG in (E) Control, (F) *ASC* KO, and (G) *CASP1*KO THP1 *NLRP3 D303N* cells were measured at 30-min intervals.

Data are shown as mean ± SD of triplicate (B) or pentaplicate (E–G) of one experiment. (A–G) Data are representative of two independent experiments. *p < 0.05, **p < 0.01, ***p < 0.001 as determined by two-way ANOVA with a post hoc test.

that caspase-1/11-independent necrotic cell death induced by NLRP3 inflammasome activation was mediated by caspase-dependent pyroptosis. Furthermore, RIPK3-dependent necroptosis occurred instead of pyroptosis when caspases were inhibited.

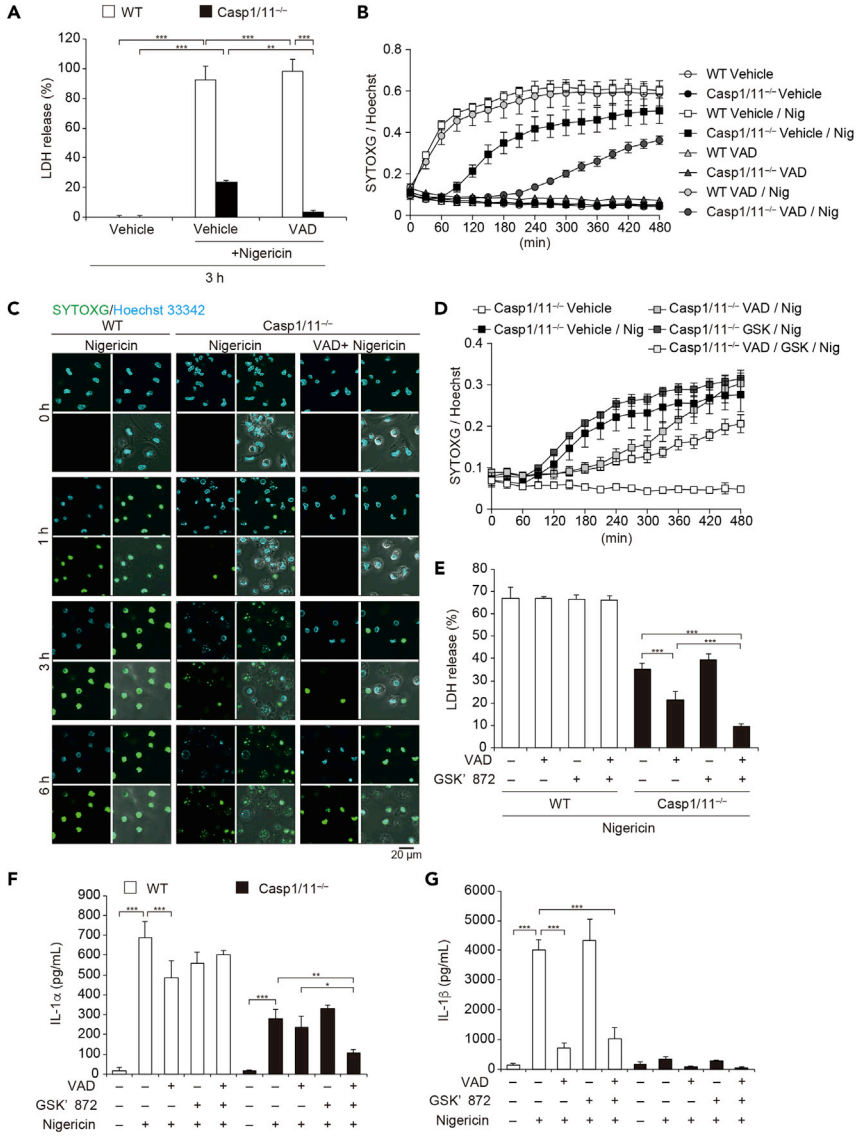

Figure 3. Other Caspases Are Involved in Caspase-1/11-Independent Necrotic Cell Induced by NLRP3 Inflammasome Activation

(A–C) Pam3CSK4-primed WT and *Casp1/11*$^{-/-}$ macrophages were pretreated with Z-VAD (20 μM) and then treated with nigericin (5 μM). (A) The levels of LDH in the supernatants were assessed 3 h after nigericin treatment. (B) Relative fluorescence units of SYTOXG were measured at 30-min intervals. (C) Images were visualized by confocal microscopy. (D–G) Pam3CSK4-primed WT and *Casp1/11*$^{-/-}$ macrophages were pretreated with Z-VAD and GSK'872 (3 μM) and then treated with nigericin. (D) Relative fluorescence units of SYTOXG were measured at 30-min intervals. (E) The levels of LDH in the supernatants were assessed. (F) The levels of IL-1α and (G) IL-1β in the supernatants were assessed by ELISA. (A, B, and D–F) Data are shown as mean ± SD of triplicate of one experiment. Data are representative of two (B, C, F, and G) or three (A, D, and E) independent experiments. *$p < 0.05$, **$p < 0.01$, ***$p < 0.001$ as determined by two-way ANOVA with a post hoc test.

GSDME Is Processed in Caspase-1/11-Independent Pyroptosis Induced by NLRP3 Inflammasome Activation

To identify the molecule that is responsible for nigericin-induced necrotic cell death in *Casp1/11*$^{-/-}$ macrophages, we assessed the processing of caspases and gasdermins. In primed WT macrophages, nigericin induced caspase-1 activation and subsequent GSDMD processing that were completely prevented in *Casp1/11*$^{-/-}$ macrophages (Figure 4A). By contrast, caspase-8 and -3 (caspase-8/3) were activated in

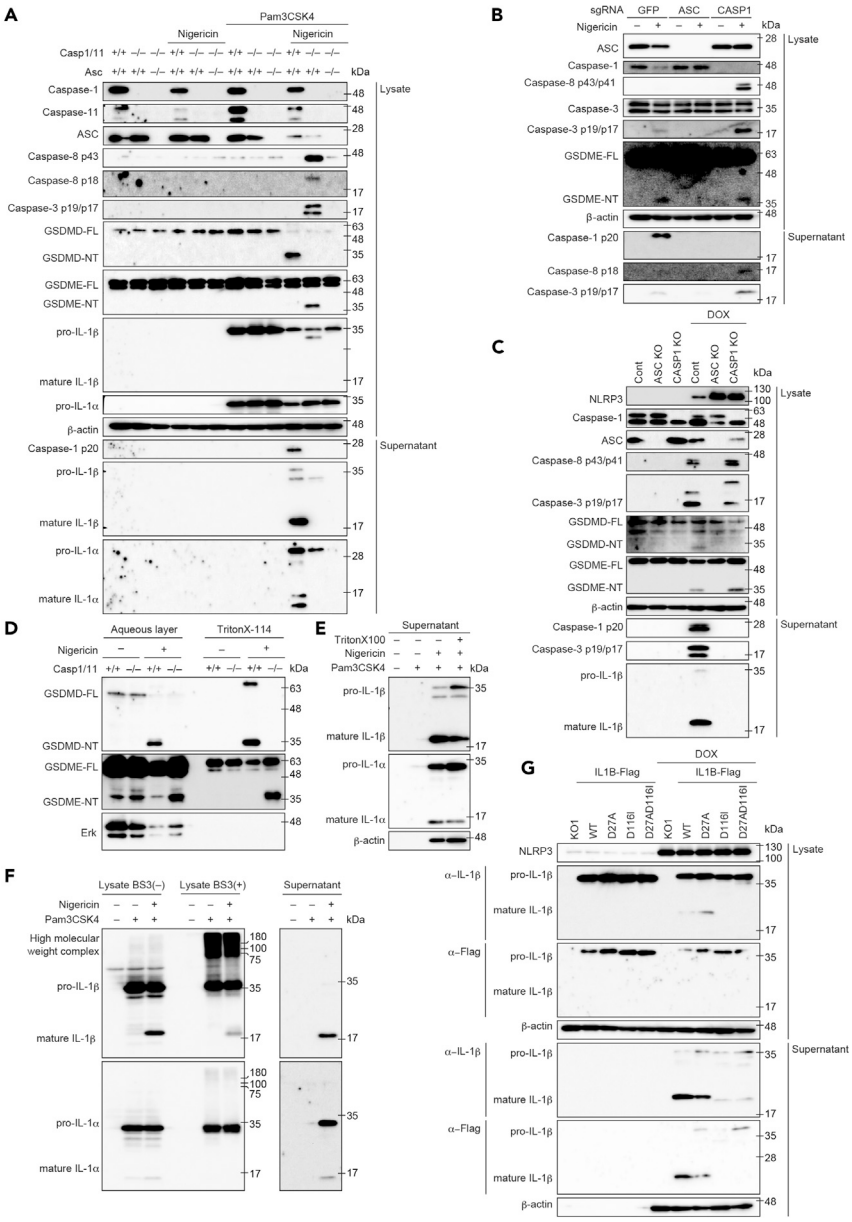

Figure 4. GSDME Is Processed in Caspase-1 Caspase-1/11-Independent Necrotic Cell Induced by NLRP3 Inflammasome Activation

(A) Primary peritoneal macrophages isolated from WT, *Casp1/11*$^{-/-}$, and *Asc*$^{-/-}$ *Casp1/11*$^{-/-}$ mice were rested or primed with Pam3CSK4 (100 ng/mL) for 18 h and then treated with nigericin (5μM) for 3 h. Lysates and supernatants were analyzed by western blot.

(B) Control, *ASC*KO, and *CASP1* KO THP1 cells were differentiated with PMA for 48 h and treated with nigericin (5 μM) for 8 h. Lysates and supernatants were analyzed by western blot.

(C) Control, *ASC*KO, and *CASP1*KO THP1 *NLRP3 D303N* cells were differentiated with PMA for 48 h and treated with DOX (1 μg/mL) for 18 h. Lysates and supernatants were analyzed by western blot.

(D) Primed WT and *Casp1/11*$^{-/-}$ macrophages were treated with nigericin for 3 h. Cells were lysed with Triton X-114 and separated into an aqueous phase and detergent phase. Each fraction was precipitated by acetone and analyzed by western blot.

(E and F) Pam3CSK4-primed WT macrophages were stimulated with nigericin. (E) After 3 h, cells were lysed with Triton X and supernatants were analyzed by western blot. (F) After 30 min, cell lysates were cross-linked with BS3 and analyzed by western blot.

(G) THP1 *NLRP3 D303N*/*hIL1B* cells were differentiated with PMA for 48 h and treated with DOX for 6 h. Lysates and supernatants were analyzed by western blot.

(A–G) Data are representative of two independent experiments.

nigericin-treated primed *Casp1/11*$^{-/-}$ macrophages. Recently, Wang et al. demonstrated that another gasdermin, GSDME/DFNA5, could be processed by caspase-3 and induce pyroptosis (Wang et al., 2017). Indeed, GSDME was apparently processed only in stimulated *Casp1/11*$^{-/-}$ macrophages, whereas neither GSDMD-NT nor GSDME-NT was observed in *Asc*$^{-/-}$*Casp1/11*$^{-/-}$ macrophages (Figure 4A). Similarly, the processing of GSDME accompanied by caspase-8/3 activation was induced in nigericin-stimulated *CASP1* KO THP-1 cells and DOX-treated *CASP1* KO *NLRP3D303N*-THP-1 cells (Figures 4B and 4C). Next, we assessed the time course of GSDME processing because the onset of nigericin-induced necrotic cell death in *Casp1/11*$^{-/-}$ macrophages was slower than that in WT macrophages. In agreement with the delayed onset of cell death, processing of GSDME strongly proceeded 1–3 h after stimulation (Figure S5A). Previous studies have suggested that NT of gasdermins binds phosphatidylinositol and translocates to plasma membrane during pyroptosis (Ding et al., 2016; Liu et al., 2016). Therefore, we assessed whether GSDMD-NT and GSDME-NT could be located in Triton X-114-soluble membrane-containing fraction. Full-length GSDMD and GSDME were distributed in the aqueous phase (Figure 4D). Although processed GSDMD-NT was detected in the Triton X-114-soluble phase in nigericin-treated WT macrophages, GSDMD-NT was not found in the same fraction of nigericin-treated *Casp1/11*$^{-/-}$ macrophages. Instead, GSDME-NT was distributed in Triton X-114-soluble phase in nigericin-treated *Casp1/11*$^{-/-}$ macrophages. These results indicate that distinct gasdermins were processed for the induction of pyroptosis in the presence or absence of caspase-1/11 during NLRP3 inflammasome activation.

Unprocessed pro-IL-1β Is Retained in Pyroptotic Cells under Caspase-1 Inhibition

Previous reports suggested that IL-1β can be processed by caspase-8 even in the absence of caspase-1 (Antonopoulos et al., 2015; Schneider et al., 2017). However, we found that mature IL-1β was only faintly detected in the lysate of stimulated *Casp1/11*$^{-/-}$ macrophages despite substantial activation of caspase-8 (Figure 4A). Instead, partially processed IL-1β (estimated molecular weight 28 kDa) was detected in lysates and supernatants of nigericin-stimulated *Casp1/11*$^{-/-}$ macrophages, indicating that mature IL-1β (p17) was not a major product of caspase-8-mediated processing. Meanwhile, although only a modest amount of pro-IL-1β was detected in supernatants of nigericin-stimulated WT macrophages, substantial amounts of mature IL-1β and IL-1α were detected in the same fraction. Therefore, we assumed that some unidentified mechanism holds unprocessed pro-IL-1β in pyroptotic cells. To assess the remaining pro-IL-1β in pyroptotic cells, WT macrophages that had undergone pyroptosis 3 h after nigericin stimulation were lysed by Triton X-100. Mature IL-1β in supernatants was not increased by cell lysis, whereas pro-IL-1β in supernatants was dramatically increased by treatment with Triton X-100 (Figure 4E). To assess the possibility that pro-IL-1β forms a molecular complex that is retained in the cytosol, a cross-link analysis with bis (sulfosuccinimidyl) suberate, disodium salt (BS3) was performed. IL-1β was detected as a higher-molecular-weight complex when reacted with BS3, whereas most IL-1α was detected as a monomer (Figure 4F). To determine whether caspase-mediated processing is needed for IL-1β release, we constructed uncleavable human IL-1β mutants by replacing Asp 27 and Asp116, which are reported to be cleavage sites of pro-IL-1β (Figure S5B). Next, lentiviral vectors encoding WT and mutated IL-1β were transduced into *NLRP3D303N*-THP-1 cells. Consistent with the results with peritoneal macrophages, selective release of mature IL-1β was detected during pyroptosis induced by NLRP3D303N (Figures 4G and S5C). As expected, mutated IL-1βD116I and D27A/D116I were not cleaved during NLRP3 inflammasome activation (Figure 4G). Moreover, mutated pro-IL-1βD116I and D27A/D116I were faintly detected in the supernatant after pyroptosis, whereas processed WT IL-1β was clearly detected in the supernatant. The mutated pro-IL-1βD116I and D27A/D116I were retained in the pyroptotic cells because treatment with Triton X-100 increased mutated pro-IL-1β in supernatants (Figure S5D). Taken together, these results suggest that pro-IL-1β forms an intracellular molecular complex and caspase-mediated processing is required for efficient IL-1β release from pyroptotic cells.

Caspase-8 Initiates GSDME Processing during NLRP3 Inflammasome Activation

Our results suggest that *Casp1/11*-independent pyroptosis during NLRP3 inflammasome activation is mediated by caspase-dependent GSDME processing. Therefore, we assessed whether Z-VAD could inhibit GSDME processing in *Casp1/11*$^{-/-}$ macrophages. Z-VAD-treatment inhibited the activation of caspases including caspase-1 in WT and caspase-8/3 in Casp1/11$^{-/-}$ macrophages, respectively (Figure 5A). Reportedly, the processing of GSDMD in WT macrophages was partially inhibited by Z-VAD-treatment (Schneider et al., 2017). In contrast, the processing of GSDME in Casp1/11$^{-/-}$ macrophages was completely abolished by Z-VAD-treatment. Because nigericin induced RIPK3-dependent necrotic cell death in Z-VAD-treated Casp1/11$^{-/-}$ macrophages (Figures 3D and 3E), we analyzed signaling of necroptosis. Nigericin stimulation

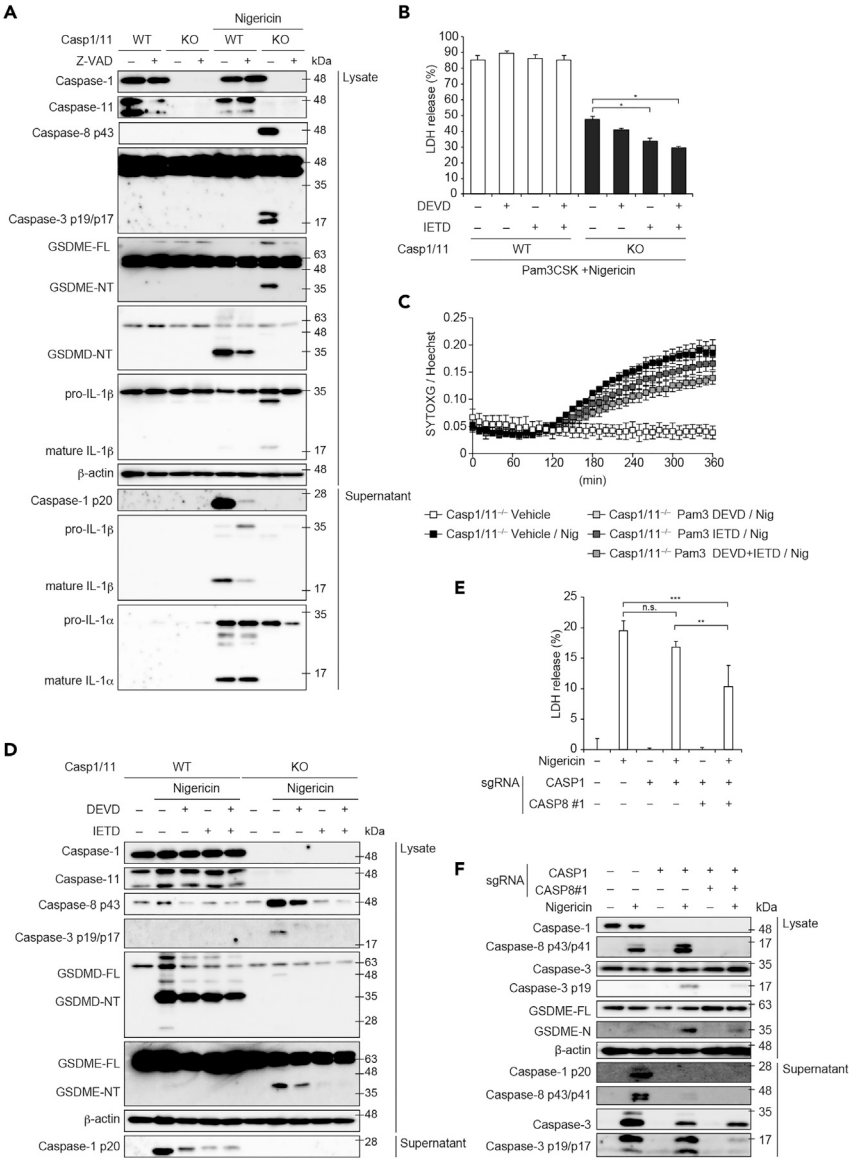

Figure 5. Caspase-8 Initiates Gasdermin E Processing during NLRP3 Inflammasome Activation

(A) Pam3CSK4-primed WT and *Casp1/11*$^{-/-}$ macrophages were pretreated with Z-VAD (20 μM) and then treated with nigericin (5 μM) for 3 h. Lysates and supernatants were analyzed by western blot.

(B–D) Pam3CSK4-primed WT and *Casp1/11*$^{-/-}$ macrophages were pretreated with DEVD and IETD (20 μM each) and then treated with nigericin. (B) After 6 h, the levels of LDH in the supernatants were assessed. (C) Relative fluorescence units of SYTOXG were measured at 10-min intervals. (D) After 3 h, lysates and supernatants were analyzed by western blot.

(E and F) Control, *CASP1* KO, and *CASP1* and *CASP8* double-KO THP1 cells were differentiated with PMA for 48 h and then treated with nigericin (5 μM) for 8 h (E) LDH release in supernatant was assessed. (F) Lysates and supernatants were analyzed by western blot.

(B, C, and E) Data are shown as mean ± SD of triplicate of one experiment. Data are representative of two (A and D–F) or three (B and C) independent experiments. *$p < 0.05$, **$p < 0.01$, ***$p < 0.001$ as determined by two-way ANOVA with a post hoc test. n.s., not significant.

promoted insoluble complex formation not only of ASC but also of RIPK3 in primed Casp1/11$^{-/-}$ macrophages (Figure S5E). The accumulation and phosphorylation of RIPK3 in insoluble fraction were further enhanced by Z-VAD treatment. Concordantly, the phosphorylation of mixed lineage kinase domain like pseudokinase (MLKL) was enhanced under Z-VAD treatment (Figure S5F). These results suggest that inflammasome activation causes MLKL-mediated necroptosis instead of gasdermin-dependent pyroptosis

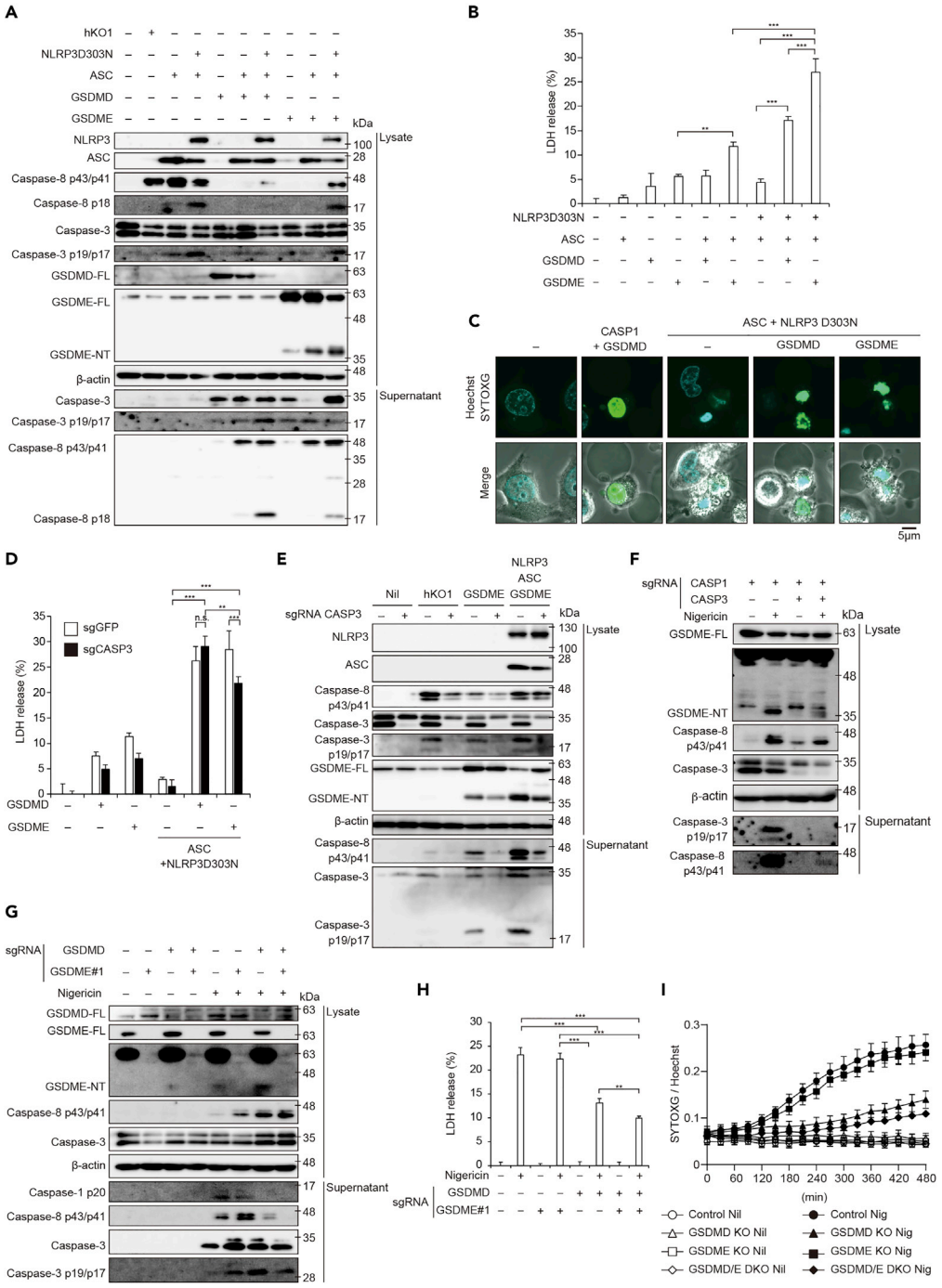

Figure 6. GSDME Serves as an Alternative Gasdermin in NLRP3 Inflammasome Activation

(A–C) HeLa cells were transfected with indicated plasmids and cultured for 24 h. (A) Lysates and supernatants were analyzed by western blot. (B) LDH release in supernatant was assessed. (C) Cells were stained with SYTOXG and Hoechst33342 and analyzed by confocal microscopy.

(D and E) *CASP3* KO HeLa cells were transiently transfected. (D) LDH release in supernatant was assessed. (E) Lysates and supernatants were analyzed by western blot.

(F) *CASP1* KO and *CASP1* and *CASP3* double-KO THP1 cells were differentiated with PMA for 48 h and then treated with nigericin (5 μM) for 8 h. Lysates and supernatants were analyzed by western blot.

Figure 6. *Continued*

(G–I) Control, *GSDMD* KO, *GSDME* KO, and *GSDMD* and *GSDME* double-KO THP1 cells were differentiated with PMA for 48 h and treated with nigericin (5 μM) for 8 h. (G) Lysates and supernatants were analyzed by western blot. (H) LDH release in supernatant was assessed. (I) Relative fluorescence units of SYTOXG were measured at 30-min intervals.

(B, D, H, and I) Data are shown as mean ± SD of triplicate of one experiment. (A–H) Data are representative of two independent experiments. $^{**}p < 0.01$, $^{***}p < 0.001$ as determined by two-way ANOVA with a post hoc test.

only when caspase-1 and caspase-8 are inhibited. To further identify the caspases that are responsible for GSDME processing, specific inhibitors of caspases were used. Although both a caspase-3 inhibitor DEVD and a caspase-8 inhibitor IETD inhibited LDH release in nigericin-treated *Casp1/11*$^{-/-}$ macrophages, the inhibitory effect of IETD was greater than that of DEVD (Figure 5B). This finding was also confirmed by an SYTOXG assay (Figure 5C). In accordance with the inhibitory effect on cell death, the processing of GSDME was abolished only in IETD-treated-*Casp1/11*$^{-/-}$ macrophages (Figure 5D). To further assess the impact of caspase-8 on caspase-1-independent necrotic cell death, we established *CASP1* and *CASP8* double-KO THP1 cells (*CASP1*/*CASP8* DKO cells) (Figure S6A). LDH release, caspase-3 activation, and GSDME processing were attenuated in *CASP1*/*CASP8* DKO cells compared with those in *CASP1* KO cells (Figures 5E and 5F). These results suggest that caspase-8 initiates GSDME processing in caspase-1-independent pyroptosis.

GSDME Serves as an Alternative Gasdermin in NLRP3 Inflammasome Activation

Next, we investigated whether NLRP3 inflammasome induces GSDME processing and subsequent pyroptosis in the absence of caspase-1. To this end, HeLa cells, which lack caspase-1 but express caspase-8 (Figure S6B), were transiently transfected with NLRP3 D303N, ASC, GSDMD, and GSDME. Reconstitution of constitutively active NLRP3 inflammasome induced caspase-8 activation, GSDME processing, and subsequent LDH release (Figures 6A and 6B). Cells reconstituted with active NLRP3 inflammasome exhibited an apoptosis-like morphology with cell shrinkage and chromatin condensation, whereas coexpression of active NLRP3 inflammasome with GSDME induced a pyroptosis-like morphology with cell swelling (Figure 6C). Since caspase-8 reportedly processes GSDMD (Orning et al., 2018; Sarhan et al., 2018), we also compared the processing of FLAG-tagged GSDMD and GSDME induced by ASC-mediated caspase-8 activation. Consistent with our findings in *Casp1/11*$^{-/-}$ macrophages, ASC-mediated caspase-8 activation preferentially promoted the processing of GSDME compared with GSDMD (Figure S6C), suggesting that NLRP3 inflammasome activation induces caspase-1-independent pyroptosis via GSDME processing. On the other hand, previous studies have suggested that caspase-3 is a responsible enzyme for GSDME processing (Rogers et al., 2017; Wang et al., 2017). To examine the role of caspase-3 in GSDME processing, we established *CASP3* KO HeLa cells (Figure S6D). When NLRP3 inflammasome was expressed with GSDME ectopically, LDH release from *CASP3* KO cells was partially attenuated compared with that from control cells (Figure 6D). Although *CASP3* deficiency attenuated GSDME processing, GSDME-NT were still detected even in the absence of caspase-3 (Figure 6E). In order to further analyze caspase-3-independent GSMDE processing by inflammasome activation, we developed *CASP1* and *CASP3* double-KO THP1 cells (*CASP1*/*CASP3* DKO cells) (Figure S6E). Nigericin-mediated inflammasome activation induced modest processing of GSDME accompanied by caspase-8 activation in *CASP1*/*CASP3* DKO cells (Figure 6F). In accordance with GSDME processing, nigericin-induced necrotic cell death in *CASP1*/*CASP3* DKO cells. (Figures S6F and S6G). These results suggest that caspase-3 contributes to, but is not indispensable for, GSDME processing.

To determine the contribution of GSDME as an alternative gasdermin to the induction of pyroptosis, we established *GSDMD* and *GSDME* DKO (*GSDMD*/*E* DKO cells) THP1 cells (Figure S6H). Caspase-8/3 activation and subsequent GSDME processing were increased in nigericin-stimulated *GSDMD* KO cells compared with those in nigericin-stimulated control cells (Figure 6G). Nigericin-induced increased membrane permeability and LDH release in *GSDMD*/*E* DKO cells were attenuated compared with those in *GSDMD* KO cells (Figures 6H and 6I), indicating that GSDME partially contributes to pyroptosis in the absence of GSDMD. These results suggest that not only GSDMD but also GSDME initiates pyroptosis via caspase-8 activation.

Pharmacological Inhibition of Caspase-1 Activation Dissociates IL-1β Release and Pyroptosis

Inflammasome-targeting drugs have been developed over the past decade for application in inflammatory diseases (Coll et al., 2015; Lee et al., 2019). In particular, both NLRP3 and caspase-1 have been regarded as possible targets for inflammasome-targeting drugs. Therefore, we investigated the effects of NLRP3-targeting MCC950 and caspase-1-targeting VX765 on IL-1α/β release and pyroptosis. Consistent

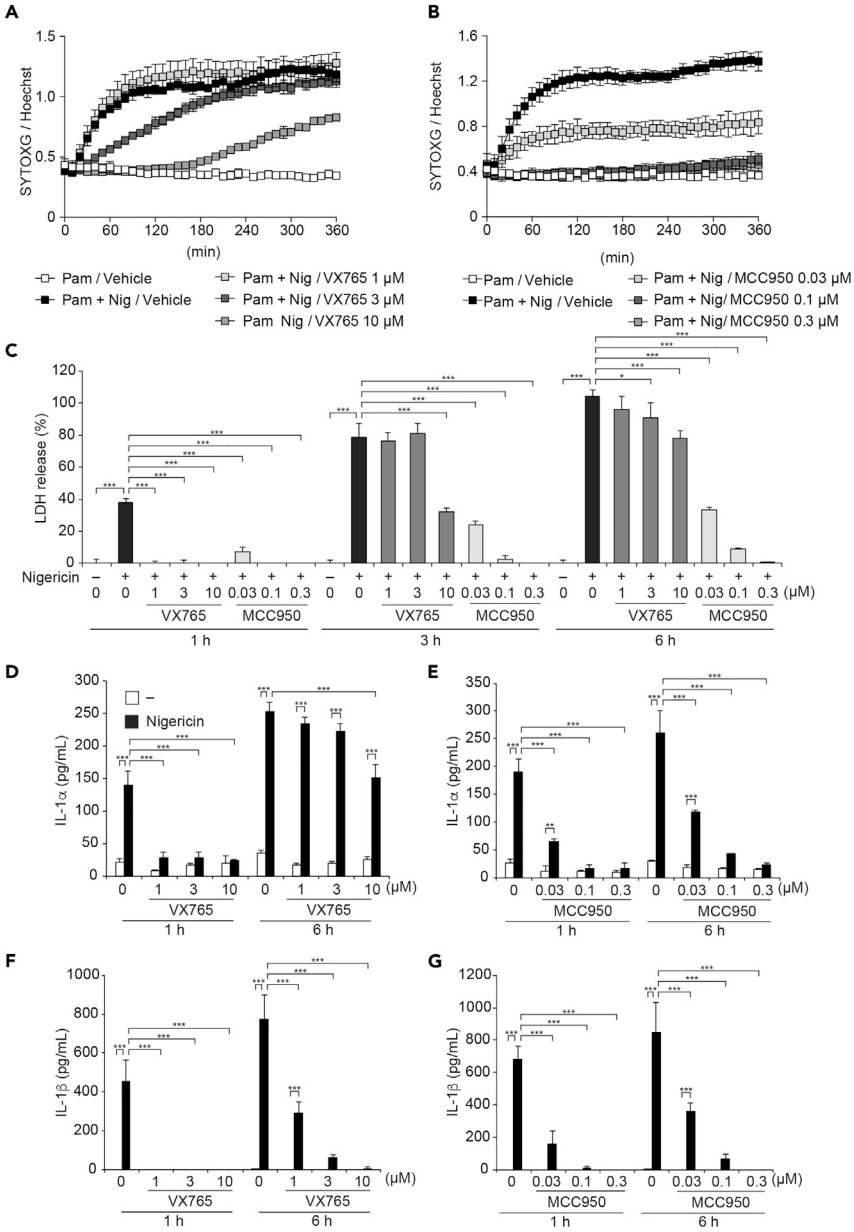

Figure 7. Pharmacological Inhibition of Casp1 Activation Dissociates IL-1β Release and Pyroptosis

(A–G) Pam3CSK4-primed WT peritoneal macrophages were pretreated with VX-765 (1–10 μM) or MCC950 (0.03–0.3 μM) for 30 min and then treated with nigericin (5 μM). Relative fluorescence units of SYTOXG in (A)VX765-treated cells and (B) MCC950-treated cells were measured at 30-min intervals. (C) The levels of LDH in the supernatants were assessed. (D and E) The levels of IL-1α and (F and G) IL-1β in the supernatants were assessed by ELISA.

(A–G) Data are shown as mean ± SD of triplicate of one experiment and representative of two independent experiments. *p < 0.05, **p < 0.01, ***p < 0.001 as determined by two-way ANOVA with a post hoc test.

with the results in Casp1/11$^{-/-}$ macrophages, VX765 dose-dependently delayed the onset of nigericin-induced cell death in Pam3CSK4-primed WT mouse peritoneal macrophages (Figure 7A). In contrast, MCC950 dose-dependently inhibited nigericin-induced cell death (Figure 7B). Although VX765-treatment completely inhibited LDH release at 1 h after nigericin treatment, VX765 failed to prevent delayed LDH release at 3–6 h after nigericin-treatment (Figure 7C). Moreover, substantial amounts of IL-1α release were detected in VX765-treated macrophages during nigericin-induced necrotic cell death (Figure 7D), whereas IL-1α release in MCC950-treated macrophages was inhibited, as well as LDH release (Figure 7E).

Unlike IL-1α release, IL-1β release was inhibited in both VX765- and MCC950-treated macrophages (Figures 7F and 7G). To clarify the mechanisms of delayed necrotic cell death under caspase-1 inhibition, we assessed the processing of gasdermins. Reduced GSDMD processing and increased GSDME processing were detected in stimulated VX765-treated macrophages (Figure S7A), indicating that the nigericin-induced necrotic cell death in VX765-treated macrophages is pyroptosis. Furthermore, we confirmed that caspase-11 was not involved in delayed pyroptosis in VX765-treated macrophages using caspase-11-mutated macrophages (Figures S7B–S7D). These results suggest that pharmacological inhibition of caspase-1 dissociates IL-1α release and IL-1β release during pyroptosis.

DISCUSSION

The major findings of this study are as follows: (1) the activation of NLRP3 inflammasome induces necrotic cell death in the absence of caspase-1/11; (2) this caspase-1/11-independent necrotic cell death is mediated by ASC; (3) ASC initiates caspase-8-mediated GSDME-dependent pyroptosis and RIPK3-mediated necroptosis; (4) IL-1α, but not IL-1β, is released during Casp1/11-independent pyroptosis; (5) unprocessed pro-IL-1β is retained in pyroptotic cells; and (6) pharmacological inhibition of caspase-1 permits selective IL-1α release during pyroptosis. These results clearly suggest that activation of the NLRP3 inflammasome induces alternative pathways of necrotic cell death accompanied by IL-1α release under caspase-1 inhibition. To initiate these necrotic cell death programs, ASC plays an essential role by activating caspase-8.

A previous study has suggested that NLRP3 inflammasome activation drives GSDMD-independent pyroptosis with increased activation of caspase-8 (Schneider et al., 2017). However, the precise mechanisms regarding GSDMD-independent pyroptosis remain unclear. In the present study, we demonstrated that ASC-mediated activation of caspase-8 promotes the processing of GSDME to induce pyroptosis in *Casp1/11*-deficient macrophages. In contrast, recent studies have suggested that caspase-8 activation during *Yersinia* infection processes GSDMD to induce pyroptosis independent of canonical NLRP3 inflammasome activation (Orning et al., 2018; Sarhan et al., 2018). However, our results clearly demonstrated that NLRP3 inflammasome-mediated activation of caspase-8 failed to process GSDMD in *Casp1/11*-deficient macrophages. Instead, NLRP3 inflammasome promoted processing of GSDME as an alternative executor of pyroptosis in *Casp1/11*-deficient macrophages. Furthermore, the active caspase-8 induced by ectopic expression of ASC preferred to process GSDME rather than GSDMD in HeLa cells. Thus, we assume that GSDME, but not GSDMD, contributes to pyroptosis mediated by NLRP3 inflammasome under caspase-1 inhibition. On the other hand, GSDME processing was detected even in the absence of caspase-3, which is responsible for GSDME processing (Rogers et al., 2017; Wang et al., 2017). In addition, selective inhibition of caspase-8 preferentially prevented GSDME processing compared with caspase-3 inhibition. Although we did not find direct evidence that caspase-8 processes GSDME, we consider that caspase-8 is essential for GSDME-mediated pyroptosis induced by NLRP3 inflammasome under caspase-1 inhibition.

Other important issues are capability of inflammasome-mediated cell death induction and resultant cell death form in the absence of caspase-1. Presumably, they might be altered depending on the priming duration and cell types. Indeed, we found that short priming duration (4 h) decreased the capability of inflammasome-mediated necrotic cell death in Casp1/11-deficient macrophages. In this regard, a previous study has suggested that c-FLIP, which functions as a modulator of caspase-8, is upregulated by toll-like receptor-mediated signals and prevents ASC/caspase-8-mediated cell death (Van Opdenbosch et al., 2017). Although it is unclear whether long priming duration downregulates c-FLIP expression, c-FLIP could be a possible candidate for regulating capability of ASC/caspase-8-mediated cell death. Meanwhile, the form of caspase-8-mediated cell death could be affected by expression profiles of GSDME. We demonstrated that ectopic expression of GSDME altered ASC/caspase-8-mediated apoptosis to pyroptosis in HeLa cells. In contrast, the previous study has suggested that inflammasome-mediated caspase-8 activation induced apoptosis in *Casp1/11*-deficient bone marrow-derived dendritic cells (Antonopoulos et al., 2015). Further analyses are required to clarify the relationship between GSDME expression patterns and ASC/caspase-8-mediated cell death in various cell types. Notably, the processing of GSDME was induced by inflammasome activation even in caspase-1-expressing THP-1 cells, whereas nigericin-induced inflammasome activation failed to induce GSDME processing in WT murine peritoneal macrophages. The processed GSDME in caspase-1-expressing THP-1 cells is dispensable for pyroptosis because a similar LDH release was detected in control and *GSDME* KO THP-1 cells. Given that, however, the inflammasome-mediated processing of GSDME is determined by expression patterns of caspase-1 and caspase-8, the cells expressing low levels of caspase-1 and high levels of caspase-8 might employ GSDME for induction of pyroptosis.

Besides pyroptosis, our results suggest that necroptosis is involved in necrotic cell death in Z-VAD-treated *Casp1/11*-deficient macrophages during NLRP3 inflammasome activation because RIPK3 inhibitor significantly prevented nigericin-mediated necrotic cell death in them. We assume that NLRP3 inflammasome initiates necroptosis only when both caspase-1 and caspase-8 are inhibited because phosphorylation of RIPK3 and MLKL was induced only in the presence of Z-VAD. Thus, GSDME-mediated pyroptosis is a primary pathway for necrotic cell death induced by NLRP3 inflammasome under caspase-1 inhibition.

Another important finding in this study is the distinct mechanisms of IL-1α and IL-1β release during pyroptosis. Although IL-1β release was abrogated by the deficiency of caspase-1/11, a substantial amount of IL-1α was released during caspase-1/11-independent necrotic cell death including pyroptosis and necroptosis. Antonopoulos et al. previously reported that, in the absence of caspase-1, caspase-8 is alternatively activated and promotes the processing of IL-1β during NLRP3 inflammasome activation (Antonopoulos et al., 2015). However, our results demonstrated that caspase-8-mediated production of mature IL-1β was extremely limited; instead, partially processed (p28) IL-1β was detected. Moreover, pro-IL-1β was retained in pyroptotic cells after NLRP3 inflammasome activation in the absence of caspase-1. Although the mechanism by which unprocessed pro-IL-1β is retained in pyroptotic cells is unclear, the size of gasdermin pores may limit the release of high-molecular-weight complex containing pro-IL-1β. According to the predicted three-dimensional structure, the estimated size of pro-IL-1β is 6–7 nm (Figure S8); therefore, pro-IL-1β monomer is small enough to be released through GSDMD pores, which range from 13 to 22 nm (Aglietti et al., 2016; Mulvihill et al., 2018). Importantly, cleavage-defective mutants of pro-IL-1β were not released from pyroptotic cells, indicating that processing of IL-1β is required for its release during pyroptosis. In this regard, Monteleone et al. reported that processed mature IL-1β interacts with phosphatidylinositol-rich plasma membrane to promote efficient IL-1β release (Monteleone et al., 2018). This mechanism may also contribute to the selective release of mature IL-1β from pyroptotic cells. On the other hand, necrotic stimuli, such as ATP, endogenous crystals, or particulate matter, induce leakage of pro-IL-1β (Gross et al., 2012). However, the pathophysiological role of released pro-IL-1β has not been determined. Multiple studies suggest that a proteinase other than caspase-1, such as neutrophil proteinases, processes pro-IL-1β to initiate inflammatory responses (Mizushina et al., 2019; Netea et al., 2015; Sadatomo et al., 2017). Thus, leakage of pro-IL-1β and subsequent processing by other proteinases could enhance inflammatory responses. In contrast, retention of pro-IL-1β in pyroptotic cells might contribute to the control of excess inflammation by preventing proteinase-mediated pro-IL-1β processing in acute inflammation.

Recently, two studies investigated the form of cell death in the absence of GSDMD. The first study suggested that NLRP3 inflammasome activation induces secondary pyroptosis in the absence of GSDMD (Schneider et al., 2017). Although the mechanism of the induction of necrotic cell death is similar to that in our study, the phenotype associated with IL-1β release is different. Since caspase-1 is still active in GSDMD-independent secondary pyroptosis (Schneider et al., 2017), processed IL-1β is released in secondary pyroptosis. In contrast, the present study suggests that pyroptosis under caspase-1 inhibition is not accompanied by IL-1β release, a key feature of pyroptosis. Thus, we defined pyroptosis under caspase-1 inhibition as incomplete pyroptosis, which lacks IL-1β release but is accompanied by IL-1α release. The second study demonstrated that caspase-1 activation induces Bid/caspase-9-dependent apoptosis in the absence of GSDMD (Tsuchiya et al., 2019). In this regard, in the present study we showed that caspase-8 functions as an initiator of caspase in GSDME-dependent incomplete pyroptosis. Taken together, the features of GSDMD-independent secondary pyroptosis or apoptosis are distinct from those of incomplete pyroptosis under caspase-1 inhibition.

IL-1α release during incomplete pyroptosis was also observed under pharmacological inhibition of caspase-1. Treatment with VX-765 failed to inhibit IL-1α release and pyroptosis during NLRP3 inflammasome activation, whereas MCC950 completely inhibited NLRP3 inflammasome-mediated responses including IL-1α/β release and pyroptosis. Although both IL-1α and IL-1β target IL-1 receptor, these cytokines have been suggested to have distinct functions (Netea et al., 2015). In particular, a recent study found that IL-1α is involved in specific processes such as thrombopoiesis after platelet loss and wound healing (Burzynski et al., 2019). Thus, pharmacological inhibition of caspase-1 may provide a new therapeutic option by permitting selective IL-1α release in inflammatory responses.

Taken together, our findings demonstrate that NLRP3 inflammasome activation induces incomplete pyroptosis accompanied by IL-1α release under caspase-1 inhibition. We assume that regulation of this complex cell death mechanism will be valuable for appropriate therapy of inflammatory diseases.

Limitations of the Study

In this study, we clarified that NLRP3 inflammasome activation induces caspase-1/11-independent necrotic cell death by activating several alternative pathways. However, this study had several limitations: (1) Although *in vitro* experiments clearly demonstrated that incomplete pyroptosis was induced by NLRP3 inflammasome activation under caspase-1 inhibition, the physiological significance of this cell death is still unclear. (2) With regard to the first issue, the processing of GSDME in an *in vivo* model was not determined in this study. (3) Caspase-8 presumably promotes the GSDME processing in the absence of caspase-3. However, we cannot exclude the possibility of GSDME processing by remaining caspase-3 because our *CASP1/CASP3* DKO cells were not cloned. At least, caspase-8 plays a pivotal role as an initiator of GSDME processing. (4) In the present study, inducers of incomplete pyroptosis are limited to nigericin and mutated NLRP3. On the other hand, lysosomal damaging stimuli such as cholesterol crystals and nanosilica particles promoted necrotic cell death independent of inflammasome. Further investigations are needed to clarify the role of incomplete pyroptosis in inflammatory responses.

METHODS

All methods can be found in the accompanying Transparent Methods supplemental file.

SUPPLEMENTAL INFORMATION

Supplemental Information can be found online at https://doi.org/10.1016/j.isci.2020.101070.

ACKNOWLEDGMENTS

This study was supported by the Japan Society for the Promotion of Science (JSPS) through Grants-in-Aid for Scientific Research (C), (18K08112, M.T.; 18K08485, T. Karasawa), the Agency for Medical Research and Development-Core Research for Evolutional Science and Technology (AMED-CREST) (M.T.), and the Ministry of Education, Culture, Sports, Science and Technology (MEXT)-supported program for Private University Research Branding Project (M.T.). We are grateful to Dr. Hiroyuki Miyoshi and Dr. Atsushi Miyawaki for providing the lentiviral vectors and Naoko Sugaya, Masako Sakurai, and Rumiko Ochiai for their technical assistance. We thank Dr. Vishva M. Dixit, Dr. Hiroko Tsusui, and Dr. Shun'ichiro Taniguchi for providing *Nlrp3*$^{-/-}$, *Casp1/11*$^{-/-}$, and *Asc*$^{-/-}$ mice, respectively.

AUTHOR CONTRIBUTIONS

Conceptualization, E.A., T. Karasawa, and M.T.; Methodology, E.A., T. Karasawa, and S.W.; Validation, R.K., H.I., E.H., and N.Y.; Investigation, E.A., T.Karasawa., S.W., T. Komada, and H.K.; Resources, E.A. and T. Karasawa; Writing - Original Draft, E.A. and T. Karasawa; Writing- Review & Editing, T. Kasahara, Y.M., and M.T.; Visualization, E.A. and T. Karasawa; Supervision, T. Komada, H.K., T. Kasahara, Y.M. and M.T.; Project Administration, E.A., T. Karasawa, and M.T.; Funding Acquisition, T. Karasawa and M.T.

DECLARATION OF INTERESTS

The authors declare no competing interests.

Received: November 13, 2019
Revised: March 11, 2020
Accepted: April 9, 2020
Published: May 22, 2020

REFERENCES

Aglietti, R.A., Estevez, A., Gupta, A., Ramirez, M.G., Liu, P.S., Kayagaki, N., Ciferri, C., Dixit, V.M., and Dueber, E.C. (2016). GsdmD p30 elicited by caspase-11 during pyroptosis forms pores in membranes. Proc. Natl. Acad. Sci. U S A *113*, 7858–7863.

Antonopoulos, C., Russo, H.M., El Sanadi, C., Martin, B.N., Li, X., Kaiser, W.J., Mocarski, E.S., and Dubyak, G.R. (2015). Caspase-8 as an effector and regulator of NLRP3 inflammasome signaling. J. Biol. Chem. *290*, 20167–20184.

Bertheloot, D., and Latz, E. (2017). HMGB1, IL-1α, IL-33 and S100 proteins: dual-function alarmins. Cell Mol. Immunol. *14*, 43–64.

Burzynski, L.C., Humphry, M., Pyrillou, K., Wiggins, K.A., Chan, J.N.E., Figg, N., Kitt, L.L., Summers, C., Tatham, K.C., Martin, P.B., et al. (2019). The coagulation and immune systems are directly linked through the activation of interleukin-1α by thrombin. Immunity *50*, 1033–1042.e6.

Coll, R.C., Robertson, A.A., Chae, J.J., Higgins, S.C., Munoz-Planillo, R., Inserra, M.C., Vetter, I., Dungan, L.S., Monks, B.G., Stutz, A., et al. (2015). A small-molecule inhibitor of the NLRP3 inflammasome for the treatment of inflammatory diseases. Nat. Med. *21*, 248–255.

Ding, J., Wang, K., Liu, W., She, Y., Sun, Q., Shi, J., Sun, H., Wang, D.C., and Shao, F. (2016). Pore-forming activity and structural autoinhibition of the gasdermin family. Nature *535*, 111–116.

Gross, O., Yazdi, A.S., Thomas, C.J., Masin, M., Heinz, L.X., Guarda, G., Quadroni, M., Drexler, S.K., and Tschopp, J. (2012). Inflammasome activators induce interleukin-1α secretion via distinct pathways with differential requirement for the protease function of caspase-1. Immunity *36*, 388–400.

Karasawa, T., and Takahashi, M. (2017). Role of NLRP3 inflammasomes in atherosclerosis. J. Atheroscler. Thromb. *24*, 443–451.

Kayagaki, N., Stowe, I.B., Lee, B.L., O'Rourke, K., Anderson, K., Warming, S., Cuellar, T., Haley, B., Roose-Girma, M., Phung, Q.T., et al. (2015). Caspase-11 cleaves gasdermin D for non-canonical inflammasome signalling. Nature *526*, 666–671.

Lamkanfi, M., and Dixit, V.M. (2014). Mechanisms and functions of inflammasomes. Cell *157*, 1013–1022.

Lee, C., Do, H.T.T., Her, J., Kim, Y., Seo, D., and Rhee, I. (2019). Inflammasome as a promising therapeutic target for cancer. Life Sci. *231*, 116593.

Liu, X., Zhang, Z., Ruan, J., Pan, Y., Magupalli, V.G., Wu, H., and Lieberman, J. (2016). Inflammasome-activated gasdermin D causes pyroptosis by forming membrane pores. Nature *535*, 153–158.

Martin, S.J. (2016). Cell death and inflammation: the case for IL-1 family cytokines as the canonical DAMPs of the immune system. FEBS J. *283*, 2599–2615.

Martin, S.J., Henry, C.M., and Cullen, S.P. (2012). A perspective on mammalian caspases as positive and negative regulators of inflammation. Mol. Cell *46*, 387–397.

Miao, E.A., Rajan, J.V., and Aderem, A. (2011). Caspase-1-induced pyroptotic cell death. Immunol. Rev. *243*, 206–214.

Mizushina, Y., Karasawa, T., Aizawa, K., Kimura, H., Watanabe, S., Kamata, R., Komada, T., Mato, N., Kasahara, T., Koyama, S., et al. (2019). Inflammasome-independent and atypical processing of IL-1β contributes to acid aspiration-induced acute lung injury. J. Immunol. *203*, 236–246.

Monteleone, M., Stanley, A.C., Chen, K.W., Brown, D.L., Bezbradica, J.S., von Pein, J.B., Holley, C.L., Boucher, D., Shakespear, M.R., Kapetanovic, R., et al. (2018). Interleukin-1β maturation triggers its relocation to the plasma membrane for gasdermin-D-dependent and -independent secretion. Cell Rep. *24*, 1425–1433.

Motani, K., Kushiyama, H., Imamura, R., Kinoshita, T., Nishiuchi, T., and Suda, T. (2011). Caspase-1 protein induces apoptosis-associated speck-like protein containing a caspase recruitment domain (ASC)-mediated necrosis independently of its catalytic activity. J. Biol. Chem. *286*, 33963–33972.

Mulvihill, E., Sborgi, L., Mari, S.A., Pfreundschuh, M., Hiller, S., and Muller, D.J. (2018). Mechanism of membrane pore formation by human gasdermin-D. EMBO J. *37*, e98321.

Netea, M.G., van de Veerdonk, F.L., van der Meer, J.W., Dinarello, C.A., and Joosten, L.A. (2015). Inflammasome-independent regulation of IL-1-family cytokines. Annu. Rev. Immunol. *33*, 49–77.

Orning, P., Weng, D., Starheim, K., Ratner, D., Best, Z., Lee, B., Brooks, A., Xia, S., Wu, H., Kelliher, M.A., et al. (2018). Pathogen blockade of TAK1 triggers caspase-8-dependent cleavage of gasdermin D and cell death. Science *362*, 1064–1069.

Rogers, C., Fernandes-Alnemri, T., Mayes, L., Alnemri, D., Cingolani, G., and Alnemri, E.S. (2017). Cleavage of DFNA5 by caspase-3 during apoptosis mediates progression to secondary necrotic/pyroptotic cell death. Nat. Commun. *8*, 14128.

Sadatomo, A., Inoue, Y., Ito, H., Karasawa, T., Kimura, H., Watanabe, S., Mizushina, Y., Nakamura, J., Kamata, R., Kasahara, T., et al. (2017). Interaction of neutrophils with macrophages promotes IL-1β maturation and contributes to hepatic ischemia-reperfusion injury. J. Immunol. *199*, 3306–3315.

Sagulenko, V., Thygesen, S.J., Sester, D.P., Idris, A., Cridland, J.A., Vajjhala, P.R., Roberts, T.L., Schroder, K., Vince, J.E., Hill, J.M., et al. (2013). AIM2 and NLRP3 inflammasomes activate both apoptotic and pyroptotic death pathways via ASC. Cell Death Differ. *20*, 1149–1160.

Sarhan, J., Liu, B.C., Muendlein, H.I., Li, P., Nilson, R., Tang, A.Y., Rongvaux, A., Bunnell, S.C., Shao, F., Green, D.R., et al. (2018). Caspase-8 induces cleavage of gasdermin D to elicit pyroptosis during Yersinia infection. Proc. Natl. Acad. Sci. U S A *115*, E10888–E10897.

Satoh, T., Kambe, N., and Matsue, H. (2013). NLRP3 activation induces ASC-dependent programmed necrotic cell death, which leads to neutrophilic inflammation. Cell Death Dis. *4*, e644.

Schneider, K.S., Gross, C.J., Dreier, R.F., Saller, B.S., Mishra, R., Gorka, O., Heilig, R., Meunier, E., Dick, M.S., Cikovic, T., et al. (2017). The inflammasome drives GSDMD-independent secondary pyroptosis and IL-1 release in the absence of caspase-1 protease activity. Cell Rep. *21*, 3846–3859.

Shi, J., Zhao, Y., Wang, K., Shi, X., Wang, Y., Huang, H., Zhuang, Y., Cai, T., Wang, F., and Shao, F. (2015). Cleavage of GSDMD by inflammatory caspases determines pyroptotic cell death. Nature *526*, 660–665.

Tonnus, W., and Linkermann, A. (2017). The in vivo evidence for regulated necrosis. Immunol. Rev. *277*, 128–149.

Tonnus, W., Meyer, C., Paliege, A., Belavgeni, A., von Massenhausen, A., Bornstein, S.R., Hugo, C., Becker, J.U., and Linkermann, A. (2019). The pathological features of regulated necrosis. J. Pathol. *247*, 697–707.

Tsuchiya, K., Nakajima, S., Hosojima, S., Thi Nguyen, D., Hattori, T., Manh Le, T., Hori, O., Mahib, M.R., Yamaguchi, Y., Miura, M., et al. (2019). Caspase-1 initiates apoptosis in the absence of gasdermin D. Nat. Commun. *10*, 2091.

Vajjhala, P.R., Lu, A., Brown, D.L., Pang, S.W., Sagulenko, V., Sester, D.P., Cridland, S.O., Hill, J.M., Schroder, K., Stow, J.L., et al. (2015). The inflammasome adaptor ASC induces procaspase-8 death effector domain filaments. J. Biol. Chem. *290*, 29217–29230.

Vanden Berghe, T., Linkermann, A., Jouan-Lanhouet, S., Walczak, H., and Vandenabeele, P. (2014). Regulated necrosis: the expanding network of non-apoptotic cell death pathways. Nat. Rev. Mol. Cell Biol. *15*, 135–147.

Van Opdenbosch, N., Van Gorp, H., Verdonckt, M., Saavedra, P.H.V., de Vasconcelos, N.M., Goncalves, A., Vande Walle, L., Demon, D., Matusiak, M., Van Hauwermeiren, F., et al. (2017). Caspase-1 engagement and TLR-induced c-FLIP expression suppress ASC/caspase-8-dependent apoptosis by inflammasome sensors NLRP1b and NLRC4. Cell Rep. *21*, 3427–3444.

Wang, Y., Gao, W., Shi, X., Ding, J., Liu, W., He, H., Wang, K., and Shao, F. (2017). Chemotherapy drugs induce pyroptosis through caspase-3 cleavage of a gasdermin. Nature *547*, 99–103.

iScience, Volume *23*

Supplemental Information

GSDME-Dependent Incomplete Pyroptosis Permits Selective IL-1α Release under Caspase-1 Inhibition

Emi Aizawa, Tadayoshi Karasawa, Sachiko Watanabe, Takanori Komada, Hiroaki Kimura, Ryo Kamata, Homare Ito, Erika Hishida, Naoya Yamada, Tadashi Kasahara, Yoshiyuki Mori, and Masafumi Takahashi

Supplemental Information

Transparent Methods

CONTACT FOR REAGENT AND RESOUCE SHARING

Requests for resources, reagents, and further information should be directed to, and fulfilled by Tadayoshi Karasawa (tdys.karasawa@jichi.ac.jp)

METHODS DETAILS

Animals

C57BL/6J mice were purchased from SLC Inc. (Shizuoka, Japan). *Nlrp3*$^{-/-}$, *Casp1/11*$^{-/-}$, and *Asc*$^{-/-}$ mice were provided by Dr. Vishva M. Dixit, Dr. Hiroko Tsusui, and Dr. Shun'ichiro Taniguchi, respectively (Kuida et al., 1995; Mariathasan et al., 2006; Yamamoto et al., 2004). *Asc*$^{-/-}$ *Casp1/11*$^{-/-}$ mice were developed by crossing *Casp1/11*$^{-/-}$ mice with *Asc*$^{-/-}$ mice. *Casp1*$^{flox/flox}$*Casp11*$^{-/-}$ mice were generated from 129 ES cells by PhoenixBio (Hiroshima, Japan) and backcrossed with C57BL/6J for 12 generations. All genetically modified mice used in this study had a C57BL/6J background. Only male mice were used to exclude influences of the female hormonal cycle. For isolation of thioglycollate-elicited macrophages, mice were injected intraperitoneally with 1 mL of 4% Brewer thioglycollate medium (211716, Becton Dickinson, Franklin Lakes, NJ), and peritoneal cells were collected 3 days after injection. The isolated cells were pooled per genotype and seeded at 1 x 10^6 cells/mL in 10% fetal calf serum (FCS)/RPMI 1640 medium. After 3 h, non-adherent cells were washed out by phosphate-buffered saline (PBS) and adherent cells were used as peritoneal macrophages. For preparation of bone marrow-derived macrophages (BMDMs), bone marrow cells were isolated from the femurs and tibias of the mice and cultured in RPMI 1640 medium supplemented with 10% FCS and 15% conditioned medium of L929 cells (ATCC, Rockville, MD) for 7 days at density of 2 x 10^6 cells/mL. All animal experiments were approved by the Use and Care of Experimental Animals Committee of the Jichi

Medical University Guide for Laboratory Animals, and carried out in accordance with the Jichi Medical University guidelines.

Cell lines

LentiX293T (Takara Bio, Shiga, Japan) cells were cultured in Dulbecco's modified Eagle's medium (DMEM; Wako, Osaka, Japan) supplemented with 10% FCS, 1 mM sodium pyruvate, and antibiotics. THP-1 cells were cultured in RPMI1640 (Sigma, St Louis, MO, USA) supplemented with 10% FCS and antibiotics. THP-1 cells were differentiated with 200 nM PMA (Wako) for 24 or 48 h. HeLa cells were cultured in DMEM supplemented with 10% FCS and antibiotics.

Plasmids

The polymerase chain reaction (PCR)-generated cDNAs encoding hKO1, human ASC, CASP1, GSDMD, GSDME, and NLRP3 were subcloned into pCDNA3.1 vector (Thermo Fisher Scientific, Waltham, MA, USA) with or without tags (N-terminal 3 x Flag or N-terminal Myc). The lentiviral vector plasmids encoding human IL1B were developed as previously described (Mizushina et al., 2019). The mutated NLRP3D303N and IL1BD27A were generated using the PrimeSTAR Mutagenesis Basal kit (Takara Bio) with the following primers: (NLRP3D303N forward, 5′-GGCTTCAATGAGCTGCAAGGTGCCTTTGACGAG-3′; NLRP3D303N reverse, 5′-CAGCTCATTGAAGCCGTCCATGAGGAAGAGGAT-3′; IL1BD27A forward, 5′-GAAGCTGCTGGCCCTAAACAGATGAAG -3′; reverse, 5′-AGGGCCAGCAGCTTCAAAGAACAAGTC -3′). To produce doxycycline-inducible expression vector, NLRP3D303N was inserted into pENTR4 and then transferred into CS-IV -TRE-RfA-CMV-KT (kindly provided by Dr. Hiroyuki Miyoshi, RDB12876, RIKEN BRC, Tsukuba, Japan) with LR clonase (Thermo Fisher Scientific).

Lentiviral preparation

LentiX293T cells were co-transfected together with LentiCRISPRv2, pLP1, pLP2, and pVSVG using PEI MAX (Polysciences, Warrington, PA, USA) to prepare the lentiviral vectors. Culture media containing the lentiviral vectors were collected 3 days after transfection. The collected media were filtered with a 0.45-μm filter and ultracentrifuged at 21,000 rpm using a SW55 Ti rotor (Beckman Coulter, Brea, CA, USA), and the pellets were resuspended in PBS containing 5% FCS. The lentivirus titer was measured using a Lentivirus qPCR Titer kit (Applied Biological Materials, Richmond, BC, Canada).

CRISPR/Cas9-mediated genome editing in THP-1 cells

ASC, *CASP1*, *CASP3*, *CASP8*, *GSDMD*, and *GSDME* genes were mutated by CRISPR/Cas9 in THP-1 cells. The sgRNA targeting each gene was designed with CRISPR direct (http://crispr.dbcls.jp) and subcloned into LentiCRISPRv2, which was a gift from Feng Zhang (Addgene plasmid #52961; http://n2t.net/addgene: 52961; RRID: Addgene_52961), or its progeny harboring blasticidin-resistant gene. For lentiviral transduction, THP-1 cells were incubated with lentiviral vectors for 16 h in the presence of 8 μg/mL polybrene (Sigma). The transduced cells were selected by incubating them with 2 μg/mL puromycin (Sigma) for at least 3 days. To produce cells with multiple mutation, the transduced cells were further selected by blasticidin (Wako).

Development of THP-1NLRP3D303N cells

THP-1 cells were transduced with CSIV-TRE-NLRP3D303N-CMV-KT lentiviral vector at MOI 300, and transduced cells were then subjected to limited dilution cloning. To produce *CASP1*KO or *ASC* KO *NLRP3D303N*-THP-1 cells, cells were transduced with LentiCRISPRv2 vector as described above and further separated by limited dilution.

Transient transfection in HeLa cells

Transient transfection was performed using Lipofectamine 2000 (Thermo Scientific). HeLa cells were seeded at 1×10^5 cells/mL and cultured for 24 h. HeLa cells were transfected with plasmids encoding NLRP3D303N, ASC, Caspase-1, GSDMD and GSDME for 6 h. After transfection, medium was changed from DMEM to Opti-MEM (Thermo Scientific).

IL-1 secretion assay

Primary peritoneal macrophages isolated from WT, *Casp1/11*$^{-/-}$, and *Asc*$^{-/-}$ *Casp1/11*$^{-/-}$ mice were seeded at 1.25×10^5 cells/well into 96 well plates. *NLRP3D303N*-THP-1 cells were seeded at 5×10^4 cells/well into 96 well plates. After indicated treatments, culture supernatants were collected and the IL-1α and IL-1β levels were measured by enzyme-linked immunosorbent assay (ELISA) using a commercial kit (R&D Systems, Minneapolis, MN, USA). The supernatants were precipitated with ice-cold acetone and resolved in 1× Laemmli buffer for western blot analysis.

LDH release assay

Primary peritoneal macrophages isolated from WT, *Casp1/11*$^{-/-}$, and *Asc*$^{-/-}$ *Casp1/11*$^{-/-}$ mice were seeded at 1.25×10^5 cells/well into 96 well plates. *NLRP3D303N*-THP-1 cells and THP-1 cells were seeded at 5×10^4 cells/well into 96 well plates. After indicated treatments, culture supernatants were collected. Hela cells were seeded at 1.25×10^4 cells/well into 96 well plates one day before the transfection. Culture supernatants were collected at 24 h after transfection. LDH released from cells was measured by a Cytotoxicity Detection kit (Roche, Mannheim, Germany) according to the manufacturer's instructions. To determine the total cellular LDH activity, cells were lysed with 2% TritonX100. L-Lactate Dehydrogenase from rabbit muscle (Roche) was used as a standard.

SYTOX Green assay

Cells were incubated with 1 μg/mL Hoechst33342 (Dojindo, Kumamoto, Japan) for 20 min, and then cultured in the presence of 100 nM SYTOX Green (SYTOXG; Thermo Fisher Scientific) for 30 min. After labeling, cells were stimulated with reagents. Fluorescence intensity was measured by using a multimode microplate reader (Spark; TECAN, Switzerland).

Live cell imaging

Peritoneal macrophages were seeded as at 2.5 $\times 10^5$ cells on an 8-well coverglass chamber (IWAKI, Shizuoka, Japan) and primed with Pam3CSK4 for 18 h. After labeling with 1μg/mL Hoechst33342 for 20 min, cells were cultured in medium containing 100 nM SYTOXG. After images were obtained at 0 h, cells were stimulated with reagents and images were captured at the indicated time points using confocal microscopy (FLUOVIEW FV10i; Olympus, Tokyo, Japan). For imaging of HeLa cells, cells were seeded at 2.5×10^4 cells on an 8-well coverglass chamber and cultured for 24 h. Cells were transiently transfected with plasmids for 6 h, and then the medium was changed to Opti-MEM and the cells were cultured for 24 h. Before the examination, cells were labeled with SYTOXG and Hoechst33342. To evaluate the nuclear size of dead cells, images of SYTOXG staining were analyzed by Image J (1.52q; National Institutes of Health, Bethesda, MD, USA).

Crosslinking assay

Cells were lysed in cross-linking buffer (20 mM phosphate buffer, pH 8.0, 150 mM NaCl, and 1% NP-40) for the cross-linking assay. After centrifugation, the supernatants were placed on ice with 2mM BS3 (Thermo Fisher Scientific) for 2 h, and the reaction was terminated by adding an excess amount of glycine.

Isolation of Triton X100-insoluble fraction

Cells were lysed in 0.5% Triton X-100 buffer (20 mM Tris HCl, pH7.4, 10 mM KCl, 1.5 mM MgCl2, 1 mM EDTA, 1 mM EGTA, 320 mM sucrose, and 0.5% Triton X-100) for 20

min, and lysates were centrifuged at 5,000xg for 10 min. The supernatants were collected as soluble fraction. The insoluble pellets were resolved in 1× Laemmli buffer for western blot analysis.

Western blot analysis

Samples were separated by sodium dodecyl sulfate-polyacrylamide electrophoresis (SDS-PAGE) and transferred to PVDF membranes. After blocking with Blocking One (NACALAI TESQUE, Kyoto, Japan) for 30 min, the membranes were incubated overnight at 4ºC with the following primary antibodies: anti-ASC (AG-25B-0006; Adipogen, Farmingdale, NY, USA), anti-β actin, (A5441; Sigma), anti-caspase-1(AG-20B-0042-C100; Adipogen), anti-caspase-1(#3866; Cell Signaling Technology, Danvers, MA), anti-caspase-3 (#9665; Cell Signaling Technology), anti-cleaved caspase-8 (#9496; Cell Signaling Technology), anti-caspase-8 (#9746; Cell Signaling Technology), anti-cleaved caspase-8 (#8952; Cell Signaling Technology), anti-caspase-11 (#14340; Cell Signaling Technology), anti-GSDMD (#50928; Cell Signaling Technology), anti-GSDMD (G7422; Sigma), anti-GSDMD (ab209845; Abcam, Cambridge, UK), anti-GSDME (ab215191; Abcam), anti-IL-1β (sc-7884; Santa Cruz Biotechnology, Dallas, TX, USA), anti-IL-1α (AF-400-SP; R&D Systems), anti-IL-1β (AF-401NA; R&D Systems), and anti-NLRP3 (AG-20B-0014; Adipogen), anti-MLKL (MABC604; Sigma), anti-phospho-MLKL (ab196436; Abcam), anti-RIP3 (#95702; Cell Signaling Technology) , anti-phospho-RIP3 (#57220; Cell Signaling Technology) antibodies. As secondary antibodies, HRP-goat anti-mouse Superclonal IgG (Thermo Fisher Scientific), HRP-goat anti-rabbit IgG (Cell Signaling Technology), HRP-rabbit anti-goat IgG (Thermo Fisher Scientific) were incubated with membrane for 1 h. After washing with TBS-Tween, immunoreactive bands were visualized by Western Blot Quant HRP substrate (TAKARA Bio) or Western BLoT Ultra Sensitive HRP substrate (TAKARA Bio).

Statistical analysis

Data are expressed as mean ± standard deviation (SD). Differences between two groups were determined by Mann-Whitney's U-test. Differences between multiple group means were determined by two-way analysis of variance (ANOVA) combined with the Tukey's post hoc test. Differences between multiple groups with repeated measurements were determined by repeated one-way ANOVA or repeated two-way ANOVA combined with the post hoc test. All analyses were performed using GraphPad Prism 6 software (Graph Pad Software, La Jolla, CA, USA). A p-value of < 0.05 was considered statistically significant.

Prediction of IL-1β diameter

The three-dimensional structure of IL-1β pro domain (1-116) was predicted by QUARK (University of Michigan, Ann Arbor, MI, USA). The obtained structures and mature IL-1β (PDB code 1I1B) were further analyzed by CRYSOL (Version 2.8.2; European Molecular Biology Laboratory, Hamburg, Germany).

Supplemental References

Kuida, K., Lippke, J.A., Ku, G., Harding, M.W., Livingston, D.J., Su, M.S., and Flavell, R.A. (1995). Altered cytokine export and apoptosis in mice deficient in interleukin-1 β converting enzyme. Science *267*, 2000-2003.

Mariathasan, S., Weiss, D.S., Newton, K., McBride, J., O'Rourke, K., Roose-Girma, M., Lee, W.P., Weinrauch, Y., Monack, D.M., and Dixit, V.M. (2006). Cryopyrin activates the inflammasome in response to toxins and ATP. Nature *440*, 228-232.

Mizushina, Y., Karasawa, T., Aizawa, K., Kimura, H., Watanabe, S., Kamata, R., Komada, T., Mato, N., Kasahara, T., Koyama, S., *et al*. (2019). Inflammasome-Independent and Atypical Processing of IL-1β Contributes to Acid Aspiration-Induced Acute Lung Injury. Journal of immunology *203*, 236-246.

Yamamoto, M., Yaginuma, K., Tsutsui, H., Sagara, J., Guan, X., Seki, E., Yasuda, K., Yamamoto, M., Akira, S., Nakanishi, K., *et al*. (2004). ASC is essential for LPS-induced

activation of procaspase-1 independently of TLR-associated signal adaptor molecules. Genes to cells : devoted to molecular & cellular mechanisms *9*, 1055-1067.

KEY RESOURCES TABLE

REAGENT or RESOURCE	SOURCE	IDENTIFIER
Antibodies		
Rabbit monoclonal anti-caspase-1 (D7F10)	Cell Signaling Technology	#3866
Rabbit monoclonal anti-caspase-3(8G10)	Cell Signaling Technology	#9665
Rabbit monoclonal anti-cleaved caspase-8	Cell Signaling Technology	#9496
Rabbit monoclonal anti-cleaved caspase-8	Cell Signaling Technology	#8592
Mouse monoclonal anti-Caspase-8	Cell Signaling Technology	#9746
Rat monoclonal anti-Caspase-11 (17D9)	Cell Signaling Technology	#14340
Rabbit polyclonal anti-GSDMD	Cell Signaling Technology	#50928
Rabbit monoclonal anti-RIP3	Cell Signaling Technology	#95702
Rabbit polyclonal anti-phospho-RIP3	Cell Signaling Technology	#57220
Rabbit polyclonal anti-GSDMD	Sigma-Aldrich	G7422
Rabbit monoclonal anti-GSDMD	Abcam	ab209845
Rabbit monoclonal anti-GSDME	Abcam	ab215191
Rabbit monoclonal anti-phospho-MLKL	Abcam	Ab196436
Mouse monoclonal anti-NLRP3	Adipogen	AG-20B-0014
Rabbit polyclonal anti-ASC	Adipogen	AG-25B-0006
Mouse monoclonal anti-Caspase-1 (p20)	Adipogen	AG-20B-0042-C100

Rabbit polyclonal anti-IL-1β	Santa Cruz	sc-7884
Goat polyclonal anti-IL-1β	R&D	AF-401-NA
Goat polyclonal anti-IL-1α	R&D	AF-400-SP
Mouse monoclonal anti-β-actin	Sigma-Aldrich	A5441
Rat monoclonal anti-MLKL	Sigma-Aldrich	MABC604
Chemicals, Peptides, and Recombinant Proteins		
MCC950	AdipoGen	AG-CR1-3615-M005
Nigericin	Invivo Gen	tlrl-nig
Pam3CSK4	Invivo Gen	tlrl-pms
Z-DEVD-FMK	MBL	4800-510
Z-IETD-FMK	MBL	4805-510
Z-VAD-FMK	MBL	4800-520
PEI MAX	Polysciences	24765-1
VX765	Selleck	S2228
GSK'872	Selleck	S8465
Puromycin	Sigma-Aldrich	P8833
Lipofectamine 2000	Thermo Fisher Scientific	11668019
SYTOX Green	Thermo Fisher Scientific	S7020
Blasticidin S Hydrochloride	Wako	029-18701
Phorbol 12-Myristate 13-Acetate	Wako	162-23591
Doxycycline Hydrochloride n-Hydrate	Wako	049-31121
Critical Commercial Assays		
Lentiviral qPCR Titration Kit	Applied Biological Materials	#LV900
Cytotoxicity Detection Kit (LDH)	Roche	11644793001
Human IL-1 beta/IL-1F2 DuoSet ELISA	R＆D Systems	DY201
Mouse IL-1 beta/IL-1F2 DuoSet ELISA	R＆D Systems	DY401
Mouse IL-1 alpha/IL-1F1 DuoSet ELISA	R＆D Systems	DY400
Experimental Models: Cell Lines		

LentiX293T	Takara Bio	Z2180N
Hela	ATCC	CCL-2
Hela *CASP3* KO	This manuscript	N/A
THP-1	ATCC	TIB-202
THP-1 *CASP1* KO	This manuscript	N/A
THP-1 *ASC* KO	This manuscript	N/A
THP-1 *CASP1* / *CASP8* DKO	This manuscript	N/A
THP-1 *GSDMD* KO	This manuscript	N/A
THP-1 *GSDME* KO	This manuscript	N/A
THP-1 *GSDMD* / *GSDME* DKO	This manuscript	N/A
THP-1 *NLRP3D303N*	This manuscript	N/A
THP-1 *NLRP3D303N CASP1* KO	This manuscript	N/A
THP-1 *NLRP3D303N ASC* KO	This manuscript	N/A
THP-1 *NLRP3D303N* / *KO1*	This manuscript	N/A
THP-1 *NLRP3D303N* / *hIL1B*	This manuscript	N/A
THP-1 *NLRP3D303N* / *hIL1BD27A*	This manuscript	N/A
THP-1 *NLRP3D303N* / *hIL1BD116I*	This manuscript	N/A
THP-1 *NLRP3D303N* / *hIL1BD27A / D116I*	This manuscript	N/A
Experimental Models: Organisms/Strains		
Mouse: C57BL/6J	SLC	N/A
Mouse: *Casp1*$^{-/-}$*Casp11*$^{-/-}$	Kuida et al., 1995	N/A
Mouse: *Asc*$^{-/-}$	Yamamoto et al., 2004	N/A
Mouse: *Asc*$^{-/-}$*Casp1*$^{-/-}$*Casp11*$^{-/-}$	This manuscript	N/A
Mouse: *Nlrp3*$^{-/-}$	Mariathasan et al., 2006	N/A
Mouse: *Casp1*$^{flox/flox}$ *Casp11*$^{-/-}$	This manuscript	N/A
Oligonucleotides		
sgRNA sequence for GFP– GAGCTGGACGGCGACGTAAA	This manuscript	N/A
sgRNA sequence for CASP1– AAGCTGTTTATCCGTTCCAT	This manuscript	N/A

sgRNA sequence for ASC– TCTTGAGCTCCTCGGCGGTC	This manuscript	N/A
sgRNA sequence for GSDMD– TGAGCGGGTAGTCCGGAGAG	This manuscript	N/A
sgRNA sequence for CASP8#1– GCCTGGACTACATTCCGCAA	This manuscript	N/A
sgRNA sequence for CASP8#2– AACATCAAGGCATCCTTGAT	This manuscript	N/A
sgRNA sequence for GSDME#1– TCTTCTGTGTCAAAACGCAC	This manuscript	N/A
sgRNA sequence for GSDME#2– GAGAAGTGTGGTGGCATCGT	This manuscript	N/A
sgRNA sequence for CASP3#1– CATACATGGAAGCGAATCAA	This manuscript	N/A
sgRNA sequence for CASP3#2– ATTATACATAAACCCATCTC	This manuscript	N/A
Mutation PCR primer for NLRP3D303N Forward– GGCTTCAATGAGCTGCAAGGTGCCTTTGACGAG	This manuscript	N/A
Mutation PCR primer for NLRP3D303N Reverse– CAGCTCATTGAAGCCGTCCATGAGGAAGAGGAT	This manuscript	N/A
Mutation PCR primer for IL1BD27A Forward– GAAGCTGCTGGCCCTAAACAGATGAAG	This manuscript	N/A
Mutation PCR primer for IL1BD27A Reverse– AGGGCCAGCAGCTTCAAAGAACAAGTC	This manuscript	N/A
Recombinant DNA		
pcDNA3.1KO1	This manuscript	N/A
pcDNA3.1 human ASC	This manuscript	N/A
pcDNA3.1 Myc(N) human CASP1	This manuscript	N/A
pcDNA3.1 human GSDMD	This manuscript	N/A
pcDNA3.1 human GSDME	This manuscript	N/A
pcDNA3.1 3xFlag(N) human GSDMD	This manuscript	N/A
pcDNA3.1 3xFlag(N) human GSDME	This manuscript	N/A

CSIV-TRE-RfA-CMV-KT	RIKEN BRC	N/A
CSIV-TRE-NLRP3 D303N-CMV-KT	This manuscript	RDB12876
CSCA-MCS	RIKEN BRC	RDB05963
CSCAKO1	Mizushina et al., 2019	N/A
CSCA human IL1BFlagHis	Mizushina et al., 2019	N/A
CSCA human IL1BD27AFlagHis	This manuscript	N/A
CSCA human IL1BD116IFlagHIs	Mizushina et al., 2019	N/A
CSCA human IL1BD27A/D116IFlagHis	This manuscript	N/A
LentiCRISPRv2	Addgene	#52961
LentiCRISPRv2 sgGFP	This manuscript	N/A
LentiCRISPRv2 sgCASP1	This manuscript	N/A
LentiCRISPRv2 sgASC	This manuscript	N/A
LentiCRISPRv2 sgGSDMD	This manuscript	N/A
LentiCRISPRv2 sgCASP3	This manuscript	N/A
LentiCRISPRBsd	This manuscript	N/A
LentiCRISPRBsd GFP	This manuscript	N/A
LentiCRISPRBsd CASP8	This manuscript	N/A
LentiCRISPRBsd CASP3	This manuscript	N/A
LentiCRISPRBsd GSDME	This manuscript	N/A
Software and Algorithms		
GraphPad Prism 6	Graph Pad Software	
Image J	National Institute of Health	1.52q
CRYSOL	European Molecular Biology Laboratory	Version 2.8.2
QUARK	University of Michigan	

Figure S1. Nigericin-induced necrotic cell death in Casp1/11$^{-/-}$ macrophages, Related to Figure 1

(A and B) Primary peritoneal macrophages isolated from WT, *Nlrp3*$^{-/-}$, or *Casp1/11*$^{-/-}$ mice were rested or primed with Pam3CSK4 (100 ng/mL) for 18 h, and then treated with nigericin (1.5 μM) for 1 h or 6 h. (A) The levels of LDH in the supernatants from WT and *Nlrp3*$^{-/-}$ macrophages were assessed. (B) The levels of LDH in the supernatants from WT and *Casp1/11*$^{-/-}$ macrophages were assessed. (C–E) Primed WT and *Casp1/11*$^{-/-}$ macrophages were labelled with Hoechst33342, and then treated with nigericin in the presence of SYTOX Green. (C and D) Images were visualized by confocal microscopy. (E) Nuclear sizes of dead cells were quantified (WT: n = 161, *Casp1/11*$^{-/-}$: n = 94). (F and G) Control and *CASP1* KO THP-1 cells were differentiated with PMA for 48 h, and then treated with nigericin (5 μM) in the presence of SYTOXG. (F) Images were visualized by confocal microscopy and (G) nuclear sizes of dead cells were quantified (Control: n=70, *CASP1* KO: n= 35). Data are shown as (A and B) mean ± SD of triplicate of one experiment or (E and G) box plot with medians indicated as horizontal bars within boxes. (C–E) Data are representative of two independent experiment. $^{**}P < 0.01$, $^{***}P < 0.005$ as determined by (A and B) two-way ANOVA with a post hoc test or (E and G) Mann-Whitney U test.

Figure S2. Caspase-1-independent necrotic cell death induced by inflammasome activation, Related to Figure 1

(A–C) Primary peritoneal macrophages isolated from WT, *Casp1/11*$^{-/-}$, and *Asc*$^{-/-}$ *Casp1/11*$^{-/-}$ mice were rested or primed with Pam3CSK4 (100 ng/mL) for 4 h and then treated with nigericin (5 μM) for 1 h, 3 h, or 6 h. (A) The levels of LDH in the supernatants were assessed. (B) The levels of IL-1β and (C) IL-1α in the supernatants were assessed by ELISA. (D) WT, *Casp1/11*$^{-/-}$, and *Asc*$^{-/-}$ *Casp1/11*$^{-/-}$ macrophages were primed with Pam3CSK4 (100 ng/mL) for 4 h and labelled with Hoechst33342. After nigericin stimulation, relative fluorescence units of SYTOXG were measured at 10-min intervals. (E) Primary peritoneal macrophages isolated from *Casp1/11*$^{-/-}$ mice were rested or primed with Pam3CSK4 (100 ng/mL) for 4 h or 18 h and then treated with

nigericin (5 μM) for 3 h or 6 h. The levels of LDH in the supernatants were assessed. (F) WT, *Casp1/11*$^{-/-}$, and *Asc*$^{-/-}$ *Casp1/11*$^{-/-}$ bone marrow-derived macrophages were primed with Pam3CSK4 (100 ng/mL) for 18 h, and then treated with nigericin (5 μM) for 1 h, 3 h, or 6 h. The levels of LDH in the supernatants were assessed. (G and H) Control, *ASC* KO, and *CASP1* KO THP-1 cells were differentiated with PMA for 48 h, and then treated with (G) Nigericin (5 μM) for 24 h or (H) Nanosilica particles (30 nm, 100 μg/mL), Cholesterol crystals (CH-C; 100 μg/mL), and Palmitic acid crystals (PA-C; 100 μg/mL) for 24 h. The levels of LDH in the supernatants were assessed. (A–G) Data are shown as mean ± SD of triplicate of one experiment. (A–G) Data are representative of two independent experiments. $*P < 0.05$, $***P < 0.005$ as determined by two-way ANOVA with a post hoc test.

Figure S3. Development of THP-1 cells expressing NLRP3D303N mutants, Related to Figure 2

(A) Schematic model of lentiviral vector encoding NLRP3D303N mutant under the TET-ON promoter. The vector encodes hKO1 under the CMV promoter. (B–D) THP1 *NLRP3 D303N* cells were differentiated with PMA for 24 h and treated with doxycycline (DOX; 10, 100, 1000 ng/mL) for the indicated period. (B) Lysates and supernatants were analyzed by western blot after 6 h of DOX treatment. (C) LDH release in supernatants was measured. (D) The levels of IL-1β in supernatants were measured by ELISA. (E) Cells were stained with 7-AAD and FITC Annexin V and analyzed by flow cytometry. (F) THP-1 *NLRP3D303N* cells transduced with control lentiviral vectors were differentiated with PMA for 48 h and treated with DOX (1 μg/mL) in the presence of SYTOX Green. Images were visualized by confocal microscopy. (G) Control and *CASP1*KO THP1 *NLRP3 D303N* cells were differentiated with PMA for 48 h, and then treated with DOX (1 μg/mL) in the presence of SYTOXG. Images were visualized by confocal microscopy and nuclear sizes of dead cells were quantified (Control: n=128, *CASP1* KO: n= 52). Data are shown as (C and D) mean ± SD of triplicate of one experiment or (G) box plot with medians indicated as horizontal bars within boxes. (B–G) Data are representative of two

independent experiments. $^{**}P < 0.01$, $^{***}P < 0.005$ as determined by (C and D) two-way ANOVA with a post hoc test or (G) Mann-Whitney U test.

Figure S4. Effect of caspase inhibition on caspase-1-independent necrotic cell death, Related to Figure 3

(A and B) *CASP1*KO THP1 *NLRP3 D303N* cells were differentiated with PMA for 48 h, and then treated with DOX (1 μg/mL) in the presence of Z-VAD (20 μM). (A) LDH release in supernatant was assessed. (B) Cells were stimulated in the presence of SYTOXG. Relative fluorescence units of SYTOXG were measured. (C) *CASP1*KO THP1 cells were pretreated with Z-VAD, Z-DEVD or Z-IETD (20 μM each) for 30 min, and treated with nigericin (5 μM) for 8 h. LDH release in supernatant was measured. (D) Primed Casp1/11$^{-/-}$ macrophages were labelled with Hoechst33342, and then treated with Z-VAD and nigericin in the presence of SYTOX Green. Images were visualized by confocal microscopy. Data are shown as mean ± SD of triplicate (A and C) or pentaplicate (B) of one experiment. (A–D) Data are representative of two independent experiments. $^{*}P < 0.05$, $^{***}P < 0.005$ as determined by two-way ANOVA with a post hoc test.

Figure S5. NLRP3 inflammasome-mediated signaling independent of caspase-1, Related to Figure 4

(A) Primary peritoneal macrophages isolated from WT, *Casp1/11*$^{-/-}$ mice were rested or primed with Pam3CSK4 (100 ng/mL) for 18 h, and then treated with nigericin (5 μM) for 1 h, 3 h, or 6 h. Lysates and supernatants were collected at indicated time points and analyzed by western blot. (B) Alignment of amino acid sequences of human IL-1β and mouse IL-1β. Cleavage sites (ASP27 and ASP116) are indicated in red. (C and D) THP1 *NLRP3 D303N /hIL1B* cells were differentiated with PMA for 48 h and treated with DOX (1 μg/mL) for 6 h. (C) LDH release in supernatant was assessed. (D) Supernatants were analyzed by western blot. (E and F) Pam3CSK4-primed *Casp1/11*$^{-/-}$ macrophages were pretreated with Z-VAD (20 μM), and then

treated with nigericin (5 μM) for 6 h. (E) Separated soluble and insoluble fractions were analyzed by western blot. (F) Lysates were analyzed by western blot. (C) Data are shown as mean ± SD of triplicate of one experiment. (C–F) Data are representative of two independent experiments.

Figure S6. Effects of ASC-mediated caspase-8 activation on GSDME processing, Related to Figure 5 and Figure 6

(A) Lysates from control, *CASP1* KO, and *CASP1* and *CASP8* double-KO THP1 cells were analyzed by western blot. (B) Lysates from Hela cells and differentiated THP1 cells were analyzed by western blot (C) HeLa cells were transiently transfected with the indicated plasmids. After 24 h, cell lysates were analyzed by western blot. (D) Lysates from control and *CASP3* KO HeLa cells were analyzed by western blot. (E) Control, *CASP1* KO, and *CASP1* and *CASP3* double-KO THP1 cells were differentiated with PMA for 48 h. Lysates were analyzed by western blot. (F and G) *CASP1* KO, and *CASP1* and *CASP3* double-KO THP1 cells were differentiated with PMA for 48 h and then treated with nigericin (5μM) for 8 h. (F) Relative fluorescence units of SYTOXG were measured at 30-min intervals. (G) LDH release in supernatant was assessed. (H) Lysates from control, *GSDME* KO, *GSDMD* KO, *GSDMD* and *GSDME* KO were analyzed by western blot. (F and G) Data are shown as mean ± SD of triplicate of one experiment. (A–G) Data are representative of two independent experiments. $*P < 0.05$, $***P < 0.005$ as determined by two-way ANOVA with a post hoc test.

Figure S7. Pharmacological inhibition of caspase-1 in peritoneal macrophages, Related to Figure 7

(A) Primary peritoneal macrophages isolated from WT mice were pretreated with VX-765 (3 or 10 μM) or MCC950 (0.1 or 0.3 μM) for 30 min, and then treated with nigericin (5 μM). After 3 h, lysates and supernatants were analyzed by western blot. (B–D) Primary peritoneal macrophages isolated from WT mice and *Casp1*$^{flox/flox}$*Casp11*$^{-/-}$ mice were pretreated with VX-765

(1–10 μM) for 30 min, and then treated with nigericin. After 3 h, lysates and supernatants were analyzed by western blot. (C) Cells were stimulated in the presence of SYTOXG. Relative fluorescence units of SYTOXG were measured. (D) LDH release in supernatant was assessed. Data are shown as mean ± SD of triplicate (D) or pentaplicate (C) of one experiment. (C and D) Data are representative of two independent experiments. $^{**}P < 0.01$, $^{***}P < 0.005$ as determined by two-way ANOVA with a post hoc test.

Figure S8. Prediction of three-dimensional structure of IL-1β prodomain, Related to Figure 4

(A) The three-dimensional structure of IL-1β prodomain (1-116) was predicted by QUARK. The predicted structures of IL-1β prodomain and mature IL-1β were further analyzed by CRYSOL to calculate the diameter.

Figure S1

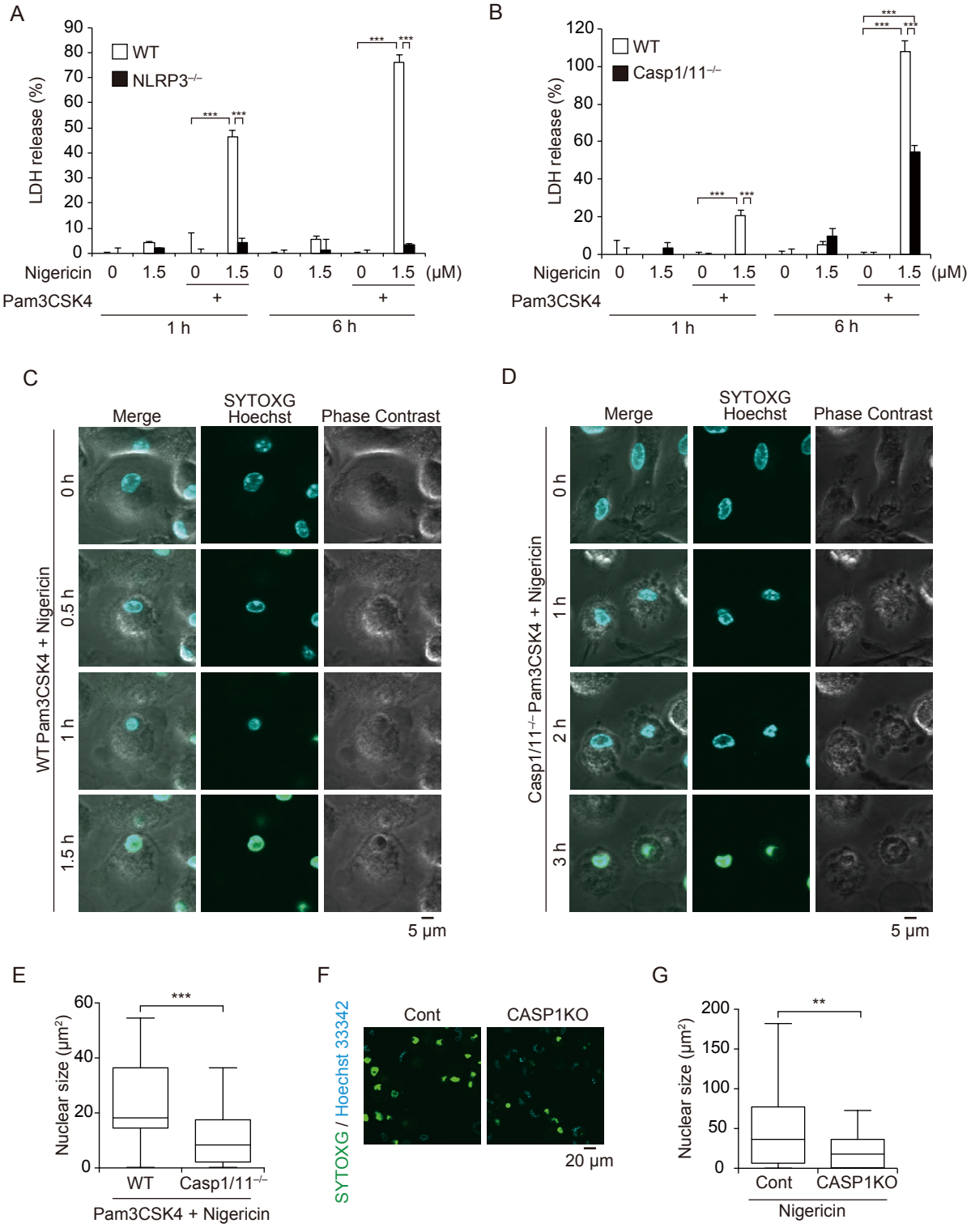
A
LDH release (%)
WT
NLRP3−/−
Nigericin
Pam3CSK4
1 h
6 h
(μM)
B
LDH release (%)
WT
Casp1/11−/−
C
Merge
SYTOXG Hoechst
Phase Contrast
WT Pam3CSK4 + Nigericin
0 h
0.5 h
1 h
1.5 h
5 μm
D
Casp1/11−/− Pam3CSK4 + Nigericin
2 h
3 h
E
Nuclear size (μm²)
WT
Casp1/11−/−
Pam3CSK4 + Nigericin
F
Cont
CASP1KO
SYTOXG / Hoechst 33342
20 μm
G
Nuclear size (μm²)
Nigericin

Figure S2

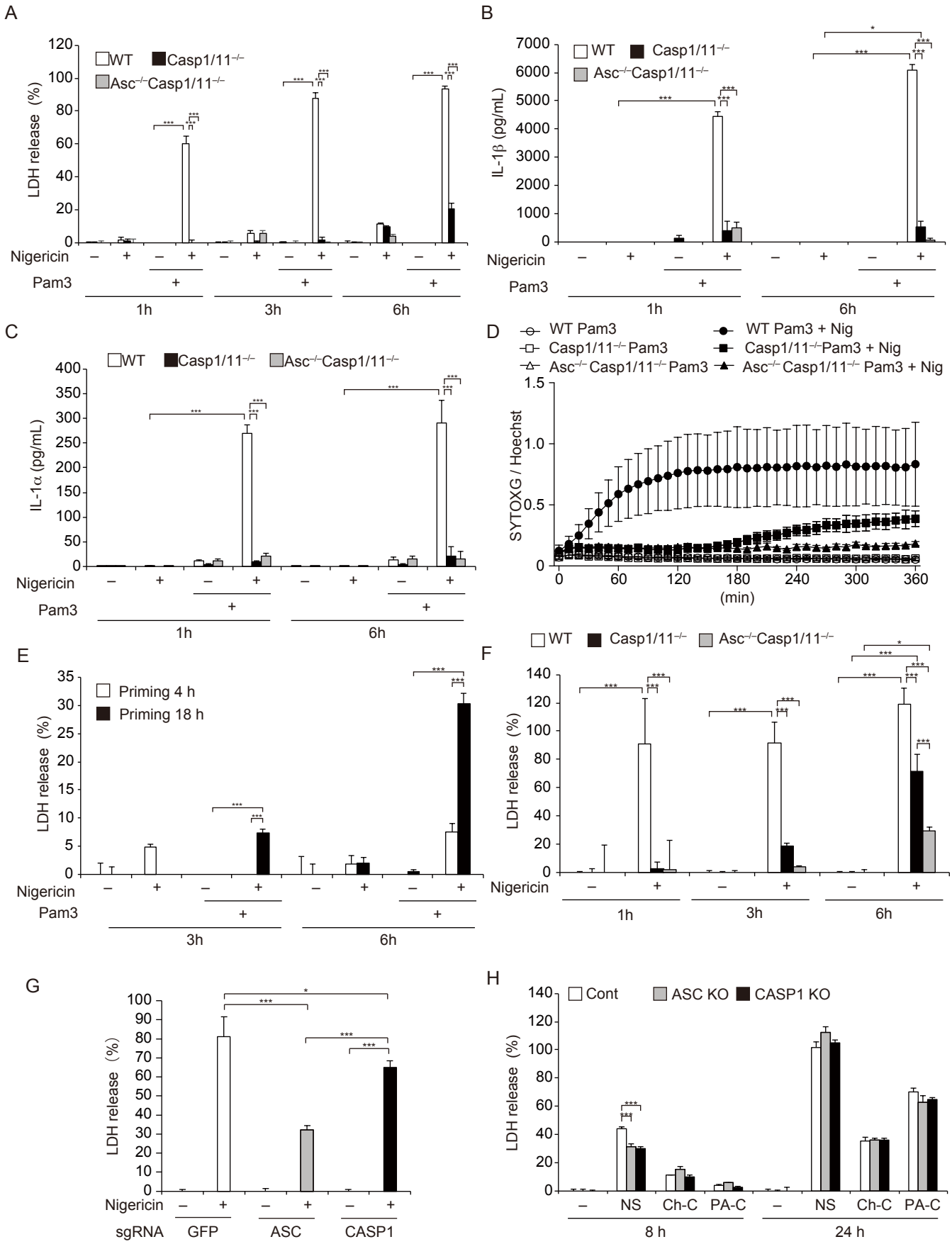
A
WT
Casp1/11−/−
Asc−/−Casp1/11−/−
LDH release (%)
Nigericin
Pam3
1h
3h
6h
B
IL-1β (pg/mL)
C
IL-1α (pg/mL)
D
WT Pam3
Casp1/11−/− Pam3
Asc−/− Casp1/11−/− Pam3
WT Pam3 + Nig
Casp1/11−/− Pam3 + Nig
Asc−/− Casp1/11−/− Pam3 + Nig
SYTOXG / Hoechst
(min)
E
Priming 4 h
Priming 18 h
3h
6h
F
G
sgRNA
GFP
ASC
CASP1
H
Cont
ASC KO
CASP1 KO
NS
Ch-C
PA-C
8 h
24 h

Figure S3

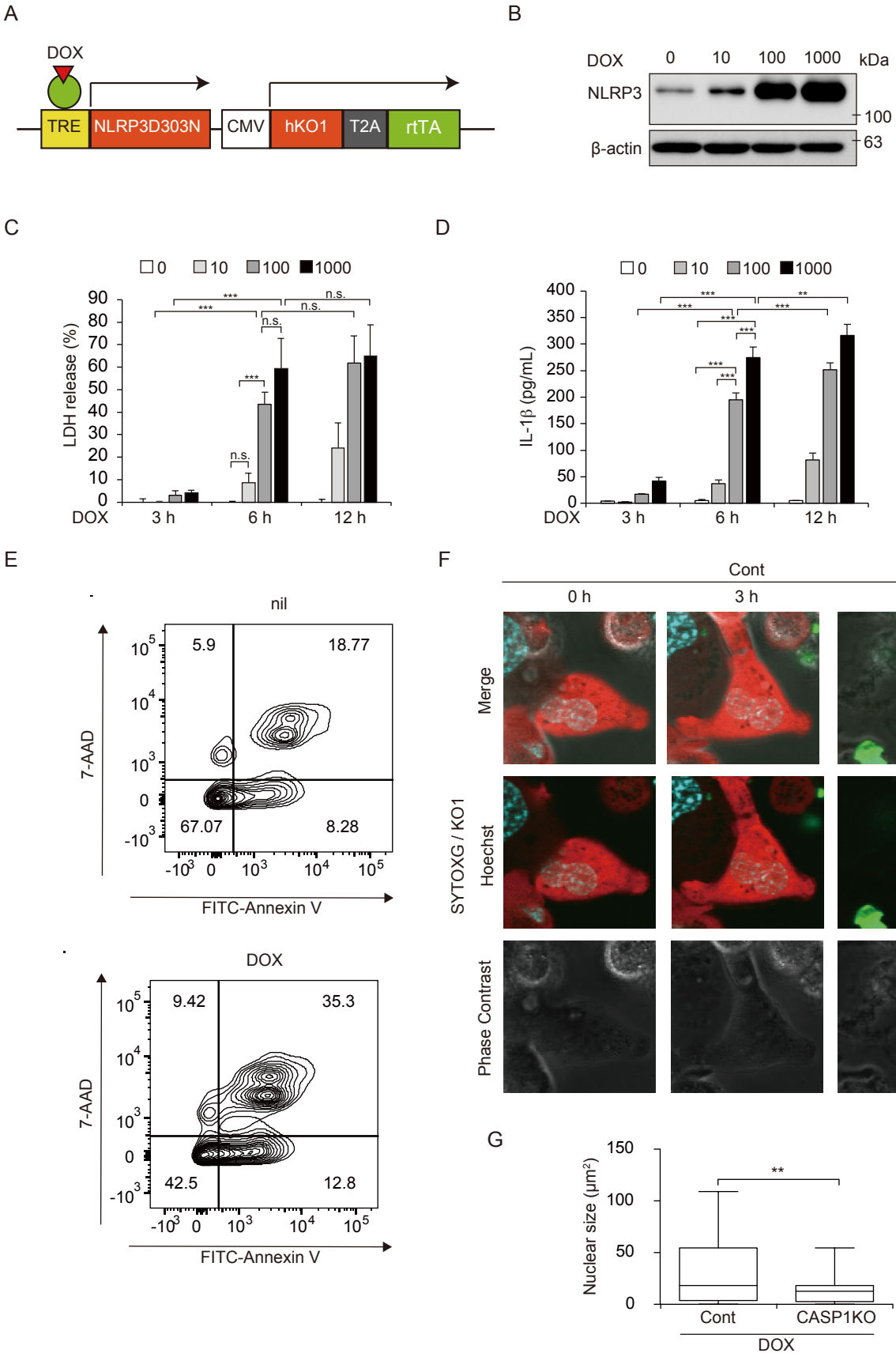
A
DOX
TRE
NLRP3D303N
CMV
hKO1
T2A
rtTA
B
DOX 0 10 100 1000 kDa
NLRP3
100
β-actin
63
C
0 10 100 1000
LDH release (%)
DOX 3 h 6 h 12 h
D
0 10 100 1000
IL-1β (pg/mL)
DOX 3 h 6 h 12 h
E
nil
5.9
18.77
67.07
8.28
7-AAD
FITC-Annexin V
DOX
9.42
35.3
42.5
12.8
7-AAD
FITC-Annexin V
F
Cont
0 h
3 h
6h
Merge
SYTOXG / KO1
Hoechst
Phase Contrast
5 μm
G
Nuclear size (μm²)
Cont
CASP1KO
DOX

Figure S4

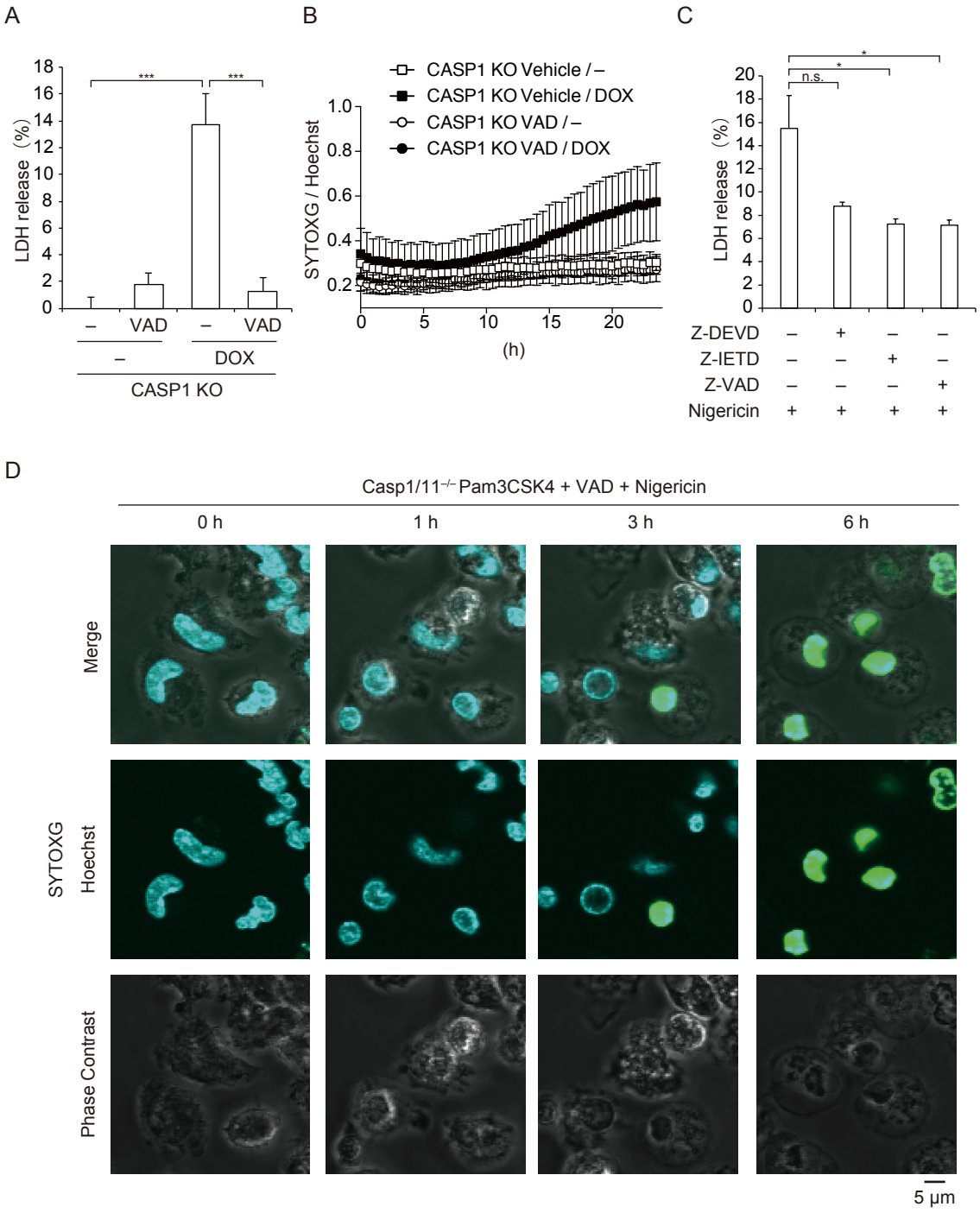
A
B
C
LDH release (%)
***
***
–
VAD
–
VAD
–
DOX
CASP1 KO
CASP1 KO Vehicle / –
CASP1 KO Vehicle / DOX
CASP1 KO VAD / –
CASP1 KO VAD / DOX
SYTOXG / Hoechst
(h)
n.s.
*
*
Z-DEVD
Z-IETD
Z-VAD
Nigericin
D
Casp1/11−/− Pam3CSK4 + VAD + Nigericin
0 h
1 h
3 h
6 h
Merge
SYTOXG
Hoechst
Phase Contrast
5 µm

Figure S5

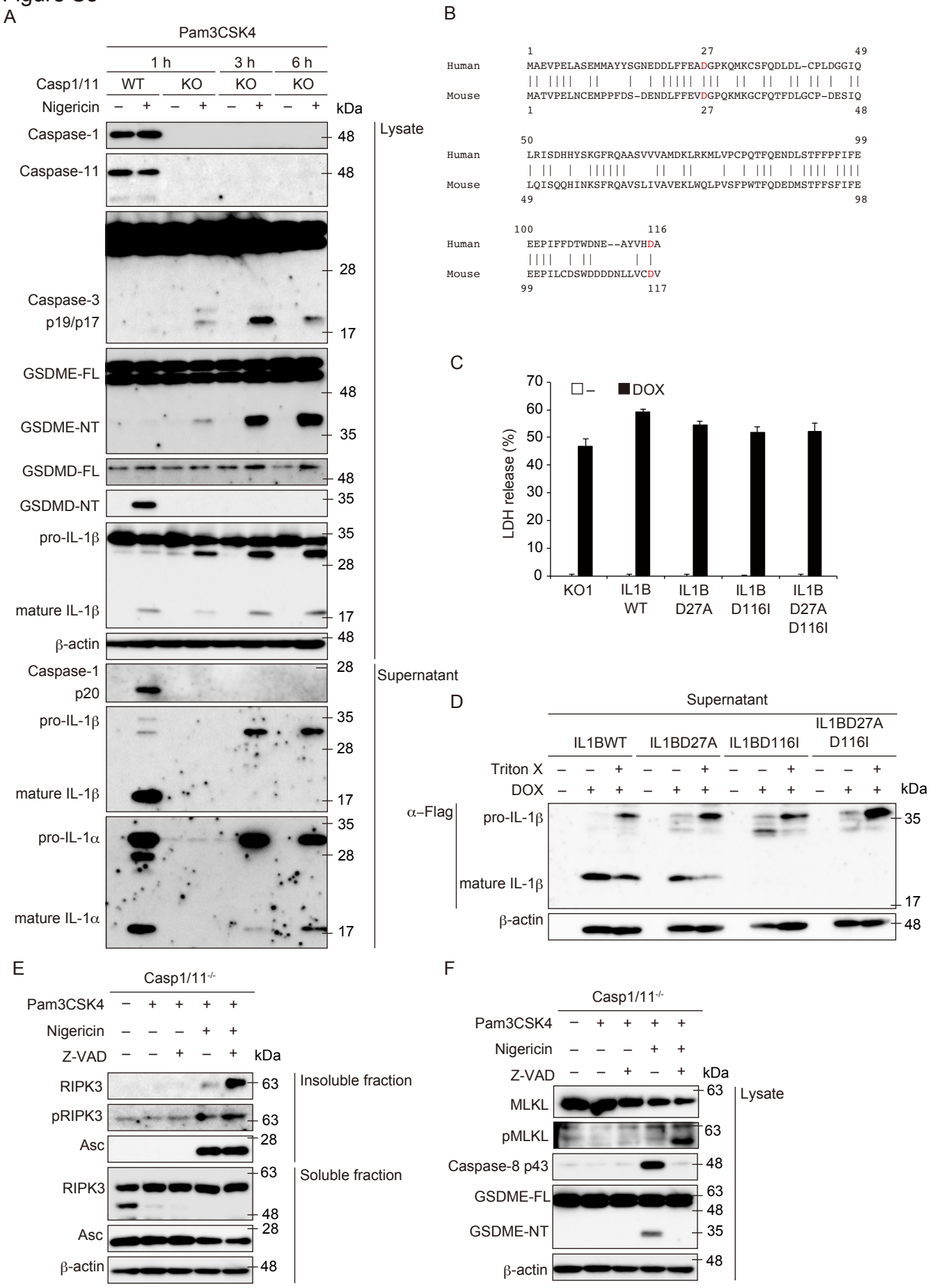
A
Pam3CSK4
1 h
3 h
6 h
Casp1/11
WT
KO
KO
KO
Nigericin
kDa
Lysate
Caspase-1
Caspase-11
Caspase-3
p19/p17
GSDME-FL
GSDME-NT
GSDMD-FL
GSDMD-NT
pro-IL-1β
mature IL-1β
β-actin
Supernatant
Caspase-1
p20
pro-IL-1β
mature IL-1β
pro-IL-1α
mature IL-1α
B
Human MAEVPELASEMMAYYSGNEDDLFFEADGPKQMKCSFQDLDL-CPLDGGIQ
Mouse MATVPELNCEMPPFDS-DENDLFFEVDGPQKMKGCFQTFDLGCP-DESIQ
Human LRISDHHYSKGFRQAASVVVAMDKLRKMLVPCPQTFQENDLSTFFPFIFE
Mouse LQISQQHINKSFRQAVSLIVAVEKLWQLPVSFPWTFQDEDMSTFFSFIFE
Human EEPIFFDTWDNE--AYVHDA
Mouse EEPILCDSWDDDDNLLVCDV
C
LDH release (%)
–
DOX
KO1
IL1B WT
IL1B D27A
IL1B D116I
IL1B D27A D116I
D
Supernatant
IL1BWT
IL1BD27A
IL1BD116I
IL1BD27A D116I
Triton X
DOX
kDa
α–Flag
pro-IL-1β
mature IL-1β
β-actin
E
Casp1/11-/-
Pam3CSK4
Nigericin
Z-VAD
kDa
Insoluble fraction
RIPK3
pRIPK3
Asc
Soluble fraction
RIPK3
Asc
β-actin
F
Casp1/11-/-
Pam3CSK4
Nigericin
Z-VAD
kDa
Lysate
MLKL
pMLKL
Caspase-8 p43
GSDME-FL
GSDME-NT
β-actin

Figure S6

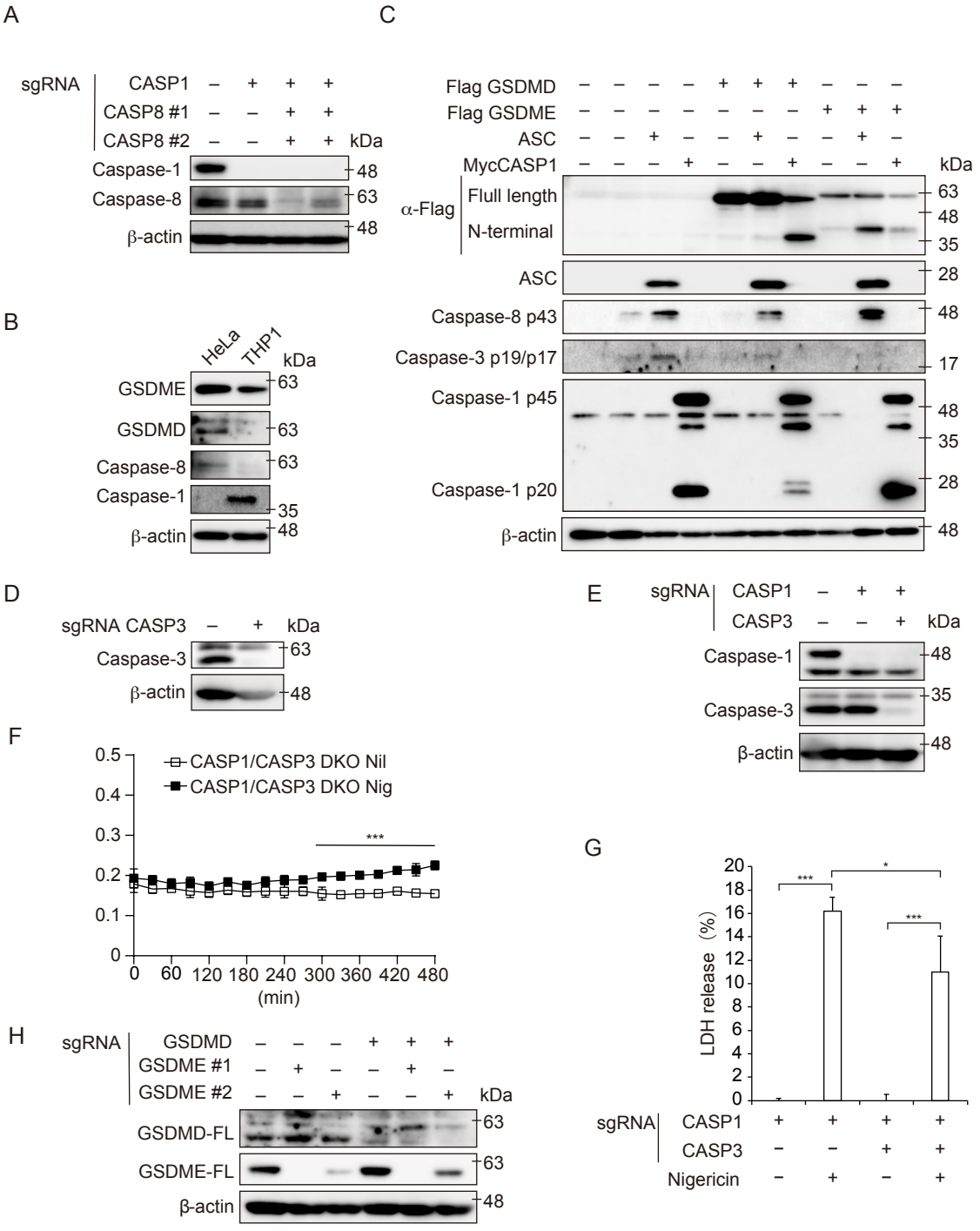
A
sgRNA
CASP1 – + + +
CASP8 #1 – – + +
CASP8 #2 – – + + kDa
Caspase-1
Caspase-8
β-actin
48
63
48
B
HeLa
THP1
kDa
GSDME
GSDMD
Caspase-8
Caspase-1
β-actin
63
63
63
35
48
C
Flag GSDMD – – – – + + + – – –
Flag GSDME – – – – – – – + + +
ASC – – + – – + – – + –
MycCASP1 – – – + – – + – – + kDa
α-Flag
Flull length
N-terminal
ASC
Caspase-8 p43
Caspase-3 p19/p17
Caspase-1 p45
Caspase-1 p20
β-actin
63
48
35
28
48
17
48
35
28
48
D
sgRNA CASP3 – + kDa
Caspase-3
β-actin
63
48
E
sgRNA
CASP1 – + +
CASP3 – – + kDa
Caspase-1
Caspase-3
β-actin
48
35
48
F
CASP1/CASP3 DKO Nil
CASP1/CASP3 DKO Nig
***
0.5
0.4
0.3
0.2
0.1
0
0 60 120 180 240 300 360 420 480
(min)
G
LDH release (%)
20 18 16 14 12 10 8 6 4 2 0
***
*
***
sgRNA
CASP1 + + + +
CASP3 – – + +
Nigericin – + – +
H
sgRNA
GSDMD – – – + + +
GSDME #1 – + – – + –
GSDME #2 – – + – – + kDa
GSDMD-FL
GSDME-FL
β-actin
63
63
48

Figure S7

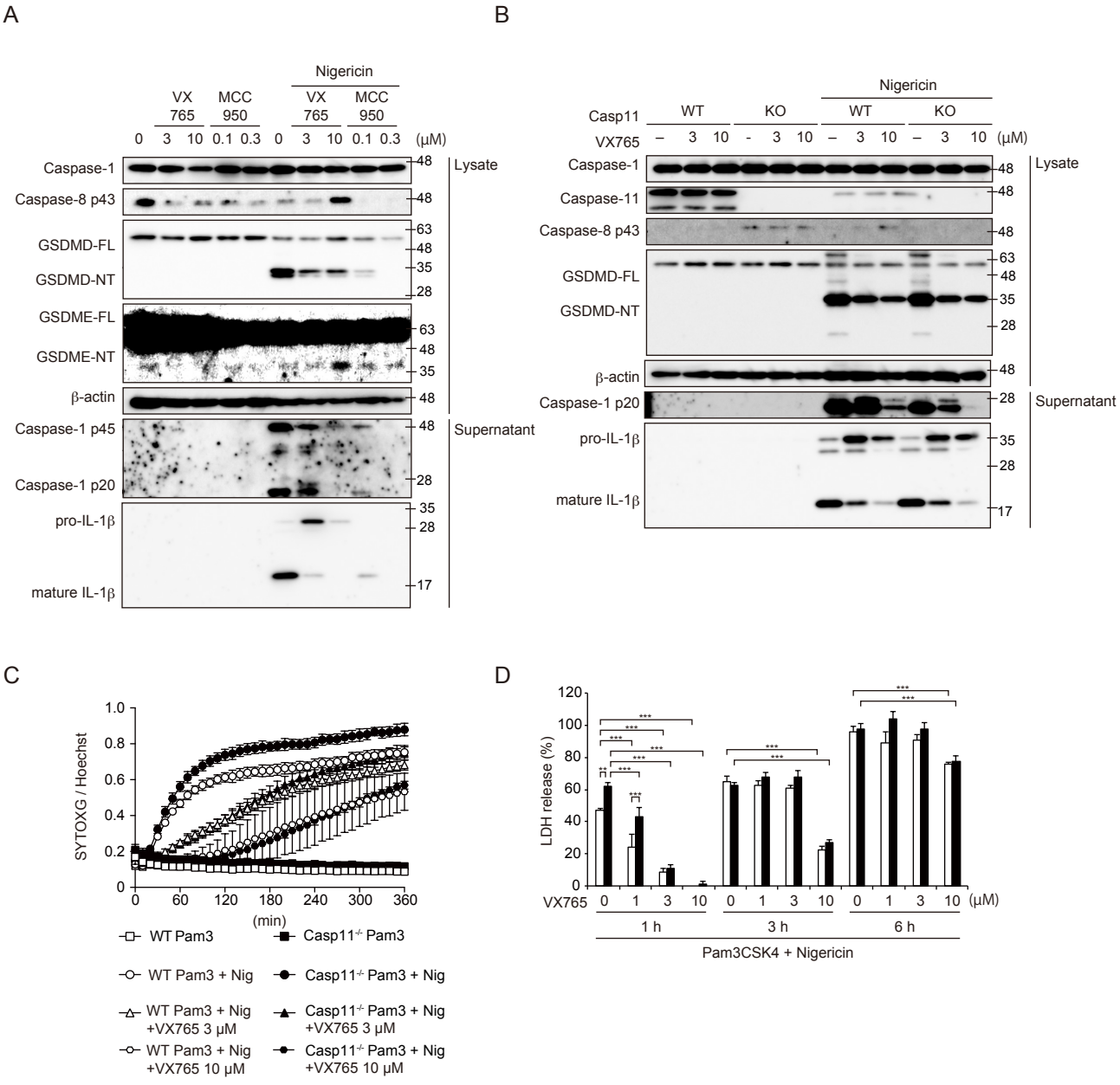
A
Nigericin
VX 765
MCC 950
VX 765
MCC 950
0 3 10 0.1 0.3 0 3 10 0.1 0.3 (μM)
Caspase-1
Caspase-8 p43
GSDMD-FL
GSDMD-NT
GSDME-FL
GSDME-NT
β-actin
Caspase-1 p45
Caspase-1 p20
pro-IL-1β
mature IL-1β
Lysate
Supernatant
B
Nigericin
Casp11
WT
KO
WT
KO
VX765
– 3 10 - 3 10 – 3 10 – 3 10 (μM)
Caspase-1
Caspase-11
Caspase-8 p43
GSDMD-FL
GSDMD-NT
β-actin
Caspase-1 p20
pro-IL-1β
mature IL-1β
Lysate
Supernatant
C
SYTOXG / Hoechst
(min)
WT Pam3
Casp11-/- Pam3
WT Pam3 + Nig
Casp11-/- Pam3 + Nig
WT Pam3 + Nig +VX765 3 μM
Casp11-/- Pam3 + Nig +VX765 3 μM
WT Pam3 + Nig +VX765 10 μM
Casp11-/- Pam3 + Nig +VX765 10 μM
D
LDH release (%)
VX765 0 1 3 10 0 1 3 10 0 1 3 10 (μM)
1 h
3 h
6 h
Pam3CSK4 + Nigericin

Figure S8

A

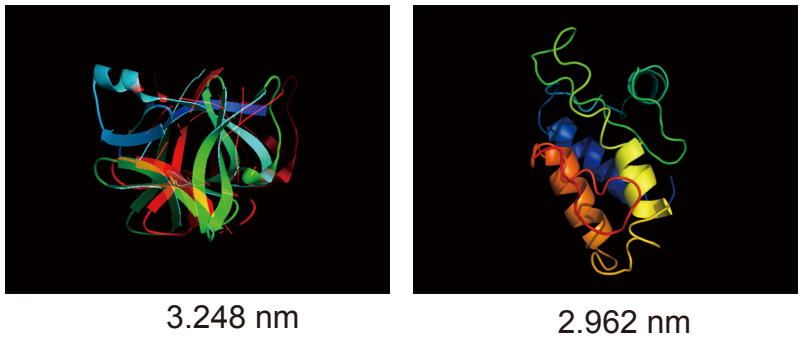
mature IL-1β
IL-1β prodomain model 1
Predicted diamter:
3.248 nm
2.962 nm
IL-1β prodomain model 2
IL-1β prodomain model 3
Predicted diamter:
2.930 nm
2.902 nm
IL-1β prodomain model 4
IL-1β prodomain model 5
Predicted diamter:
2.994 nm
2.876 nm